Carbon-based structures for electrodes: from synthesis to simulations. An overview.

Relatore: Candidato:

    Giancarlo Cicero   Giuseppe Nicastro

Correlatore:

    Federico Raffone

«Diceva Bernardo di Chartres che noi siamo come nani sulle spalle di giganti, così che possiamo vedere più cose di loro e più lontane, non certo per l'acume della vista o l'altezza del nostro corpo, ma perché siamo sollevati e portati in alto dalla statura dei giganti.»

Giovanni di Salisbury, *Metalogicon* (III, 4)

A mia Madre, che ha sempre fatto di me un suo enorme vanto.

A mio Padre, il mio unico, grande, vero Eroe.

Grazie di tutto e scusatemi per ognuno dei miei sbagli. Spero un giorno di riuscire a darvi indietro almeno un po' di quello che voi avete dato a me. Vi voglio e vi vorrò sempre bene.

TABLE OF CONTENTS

Introduction

Electrodes are one of the fundamental components in any system that aims to utilise and harness the energy and flux of electrons. Whether we are talking about energy storage systems, supercapacitors or simple transistor circuits, electrodes are required to allow the collection and movement of electric current. In recent decades, among the various materials used in the manufacture of electrodes, carbon has been one of the increasingly popular elements, due to the versatility of structures that can be realised and the numerous advantages in terms of cost and control of parameters affecting performance. After introducing the description and characterisation of supercapacitors as harvesting devices, this thesis work sets itself the task of analysing the various carbon-based electrode structures, examining the characteristic parameters and their impact on the devices involved, investigating the simulative and experimental methods used in their realisation, in order to obtain an overview of the state of the art and future technological prospects.

CHAPTER 1:
SUPERCAPACITORS AS HARVESTING SYSTEMS

1. 1 Introduction to Supercapacitors

Nowadays society requires increasing amount of energy production due to large consumption, both in industry application and for household use. The increase in world population and standard of living results in increasingly use of electronic devices, which form the basis of the complex global automation and communication network. The use of electrical energy is also increasingly driven by the political objective of reducing the use of fossil fuels in order to safeguard the planet's climate. Consequently, harvesting systems, that enable the storage of energy and electrical power, assume a primary role in view of future societal and technological development. In recent decades, Supercapacitors, harvesting systems that are halfway between conventional capacitors and classic batteries, have become increasingly important. Supercapacitors provide hundreds to many thousands of times more power in the same volume than batteries, but they are not capable of storing the same amount of charge, which is usually between 3 and 30 times lower. This makes Supercapacitors excellent devices for those applications that require a burst of power without much stored energy [14]. By means of the Ragone Plot (plot relating power and energy densities) [1], it is possible to see that supercapacitors have an energy density of between 10 and 100 W hkg^{-1}, which is greater than conventional capacitors but lower than conventional batteries, and a power density of between 500 and 10,000 W kg^{-1}, which is greater than batteries but lower than capacitors.
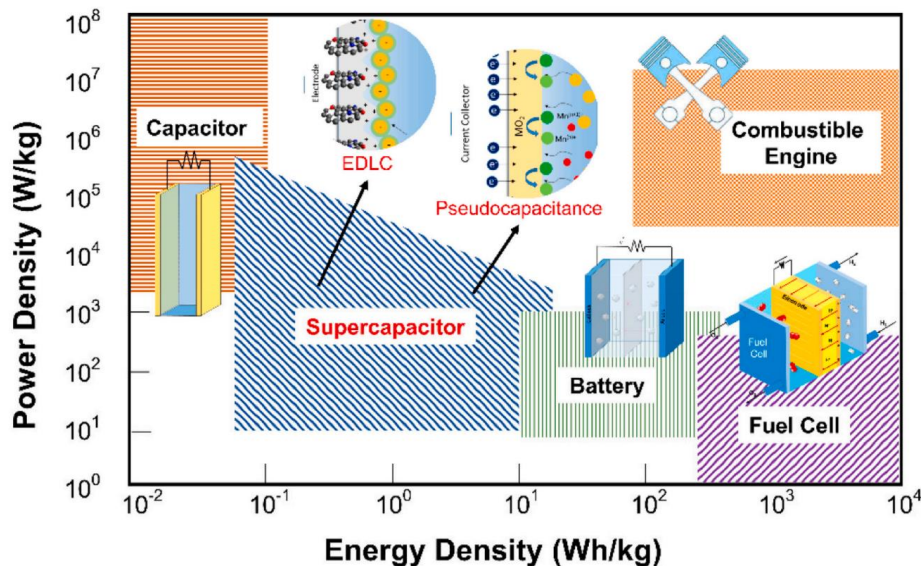
Figure 1. Ragone plot of energy storage device: Power density versus Energy density [1].

Supercapacitors have a number of advantages [1,14]:

- They can charge and discharge in few seconds [1,14];

- They have great long-life cycles; through a charging mechanism that does not involve irreversible chemical reactions, but physically stores charge at the surface of the electrodes in a double layer, Supercapacitors can withstand millions of charge/discharge cycles. This makes it possible to exceed the normal life cycle of batteries, which currently consists of a few hundred cycles. Furthermore, the high reversibility of this mechanism does not produce changes in the volume of the electrodes, eliminating the bulging typical of redox reactions occurring in the bulk of the active battery material. On the other hand, the main disadvantage of this charging mechanism is that the operating voltage must be kept low in order to avoid chemical decomposition of the electrolyte [1,14];

- Wide operating temperature range: supercapacitors can achieve high power performance even below -40°C, which is not possible with current batteries, and are also safer in high-power charge/discharge cycles. Furthermore, as they are not based on chemical charge storage mechanisms, they do not undergo metal plating, a phenomenon that afflicts normal batteries, causing degradation or the formation of short circuits resulting in uncontrollable, and potentially dangerous, reactions [1,14].

- relatively low cost [1,14];

- higher safety [1,14];

- eco-friendliness [1,14].

That is why they are among the most important devices and are subject to continuous studies to increase and improve their characteristics.

Characteristics	Capacitor	Supercapacitor	Battery
Specific energy (W h kg^{-1})	< 0.1	1–10	10–100
Specific power (W kg^{-1})	$\geqslant 10,000$	500–10,000	< 1000
Discharge time	10^{-6} to 10^{-3}	s to min	0.3–3 h
Charge time	10^{-6} to 10^{-3}	s to min	1–5 h
Coulombic efficiency (%)	About 100	85–98	70–85
Cycle-life	Almost infinite	$> 500,000$	about 1000

Table 1 Comparison table among selected electrochemical energy storage technologies [14].

Comparison parameter	Battery	Supercapacitor
Storage mechanism	Chemical	Physical
Power limitation	Reaction kinetics, mass transport	Electrolyte conductivity
Energy storage	High (bulk)	Limited (surface area)
Charge rate	Kinetically limited	High, same as discharge
Cycle life limitations	Mechanical stability, chemical reversibility	Side reactions

Table 2 Comparison between batteries and supercapacitors [14].

A supercapacitor basically consist of two electrodes divided by a separator. If the electrodes are identical, we have a symmetrical supercapacitor cell, otherwise an asymmetrical supercapacitor cell. The separator prevents contact between the electrodes and is made of a material that, when immersed in the electrolyte, is permeable to the electrolyte ions and allow the transfer of charge and, in order to

achieve high performance, requires simultaneously high electrical resistance, high ionic conductance and low thickness [14].

The electrolyte used in the supercapacitive cell influences the choice of separator: polymer separators are generally used with organic electrolytes while ceramic or glass fibre separators with aqueous electrolytes. Electrolyte conductivity will strongly depend on the equivalent series resistance (ESR) of the cell. Furthermore, the potential breakdown of the electrolyte at one of the electrodes will limit the voltage reachable by the supercapacitor: aqueous electrolytes typically have a breakdown voltage around 1V, which is significantly lower than that achievable with an organic electrolyte (3V), but have a higher conductivity, (desirable in high-power devices). Aqueous electrolytes are also less expensive and easier to handle [14].

In supercapacitors, as with simple capacitors, the capacitance will be given by the relation $C = \frac{\varepsilon_r \varepsilon_0 A}{d}$, where ε_r is the dielectric constant of the electrolyte, ε_0 the dielectric constant in vacuum, A the accessible surface area of the electrode and d the effective thickness of the double layer. The stored energy will then be $E = \frac{1}{2} C V^2$, where V is the cell voltage. The stored energy is thus proportional to both the capacitance of the device and the square of the applied voltage, therefore, to increase the energy density of the cell, the capacitance and the voltage applied to the cell should be maximised [14]. Therefore, the thickness of the double-layer, the surface area of the electrode and the dielectric material used are factors influencing the increase in capacitance and, thus, the choice of electrode material is essential to control the electrochemical properties of the supercapacitor. Generally, it is possible to modify electrodes by changing the pore size or adding functional groups or heteroatoms such as oxygen and nitrogen [1]. Changing the pore size of the electrode material leads to an increase in surface area, but alone it does not guarantee an increase in capacitance, indeed, it is necessary for the pore size to be similar to that of the ions. An additional contribution to increasing capacity is given by the addition of functional groups and heteroatoms that can increase wettability. Moreover, as we have seen, an increase in the voltage applied to the cell causes an increase in energy density, but an excessive value may cause chemical decomposition of the electrolyte. The voltage is therefore chosen according to the electrolyte involved in the cell. The most commonly used electrolytes are aqueous ones such as potassium hydroxide (KOH), sulphuric acid (H_2SO_4), potassium chloride (KCl) and sodium hydroxide (NaOH), which have a low potential window (approx. 1V): this explains the low energy density of supercapacitors and, as an alternative, other types of electrolytes with higher potential, such as organics (voltage range between 1V and 2.7V) or ions (voltage

over 3V), can be used [1]. The maximum instantaneous power that a supercapacitor is capable of releasing depends on the applied voltage and the internal resistance R: $P_{max} = \frac{V^2}{4R}$. Since the equivalent internal series resistance (ESR) must be minimised, particular attention must be given to the contact resistance between the active material and the current collector. Indeed, it would be convenient to treat the surface of the current collector before coating it with the active material. In fact, surface treatments can decrease the ohmic drop at the interface between active material and current collector and then, by using nanostructured current collectors with an increased contact area, the active material/ current collector interface can be further controlled [14].

1.2   Classification of Supercapacitors

Supercapacitors are characterised by two possible energy storage mechanisms and, in this way, we can distinguish two macro categories of capacitive behaviour. In addition, it is possible to combine the two mechanisms to obtain a third category of supercapacitors.

1.2.1.   EDLC

Electrical double layer capacitors (EDLC) have a pure electrostatic charge stored at the electrode-electrolyte interface. Due to the limited charge storage area and the geometric restraints given by the distance of separation between the two charged plates, classical capacitors store relatively little energy. EDL-based supercapacitors can store much more energy due to the large surface area and a charge separation distance of atomic range [2]. This type of supercapacitors uses nanoporous materials with a high specific surface area (>1000 m^2g^{-1}) as active materials for the electrode, thus achieving large capacitances compared to electrostatic capacitors. The material chosen for the electrodes is usually nanoporous carbon, due to its easy availability, ease of industrial production and relative low cost [2,14]. EDLCs are based on the formation of an electrical double-layer, a structure obtained when a charged object is immersed in a liquid. In the liquid, near the surface of the object, counter charges are concentrated, which balance the charged surface. Various models can be used to study what happens at the interface between liquid and solid [14].

1.2.1.1   Helmoltz Model

The Helmoltz model is the first approximation for modelling the spatial charge distribution at the interface of a double layer. The charges present in the solid electronic conductor are neutralised by ions of opposite sign spaced by an amount equal to the distance between the surface and the centre of the ion. The Helmholtz model consist of rigid layers that counterbalance the charges of the solid conductor. It is the most simplified theory to explain the phenomenon and therefore needs to be extended for a description more faithful to reality [14].

1.2.1.2   Gouy–Chapman or diffuse model

According to this model, in a liquid in which a charged solid is immersed, the same amount of ionic charges of opposite sign will be formed, but these ions will not be strongly bound to the solid's surface. Diffusion of these ions in solution into the liquid phase will occur until the counter potential generated by their movement reduces this tendency. The thickness of the diffusion layer will be partially characterise by the kinetic energy of ions. According to this theory, the concentration of ions in solution near the surface follows the Boltzmann distribution. However, the predictions fail for highly charged double layers, where the measured thickness is greater than the calculated one. Furthermore, the model assumes that ions are charged points and that they can approach the surface without limit, which is actually false [14].

1.2.1.3   Stern model

The Stern model considers ions of finite size to be limited in their approach to the surface. In contrast to the Gouy-Chapman model in which the ions closest to the surface are at a certain distance d, in the Stern model it is assumed that there can be ions absorbed by the surface of the electrodes within this space called the Stern layer. In this layer there are specifically absorbed ions, which form the so-called inner Helmholtz plane, and non-specifically absorbed counter ions, which form the outer Helmholtz plane. The Stern model is thus a combination of the two previous models [14].
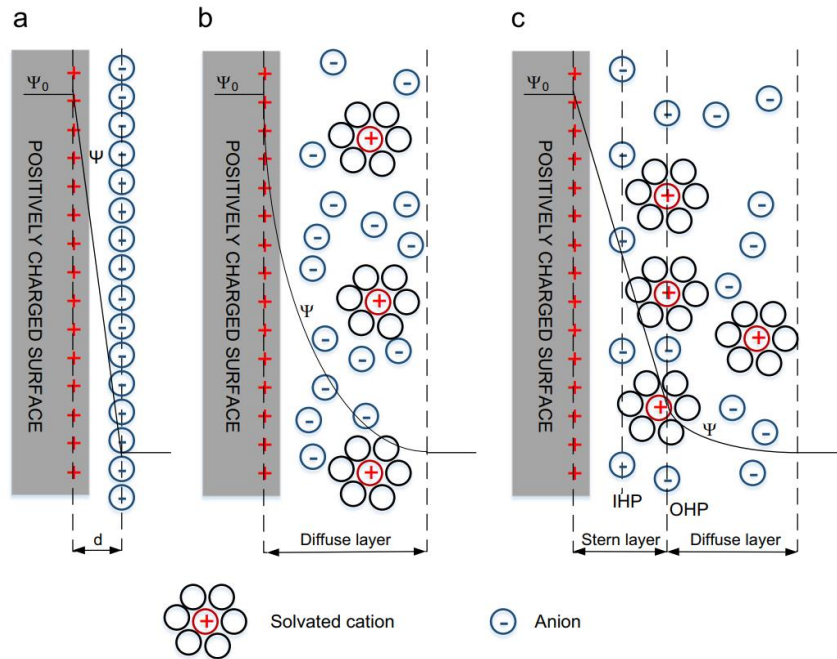
Figure 2. Schematic representation of the EDL models, (a) the Helmholtz model, (b) the Gouy–Chapman model, and (c) the Stern model [14].

1.2.1.4 Electrical Double Layer in supercapacitors

Although the models just described give a satisfactory representation of the electrical double layer on flat surfaces, they are unable to describe the actual charge distribution in nanoporous electrodes used in supercapacitors. The features of the electroabsorption of ions in porous media make the charge storage process extremely complex, also considering the absence of a complete understanding of the behaviour of ions in nanoporous structures. In a charged supercapacitor, the electrons move from the positive electrode to the negative electrode via an external circuit, as a result, the cations of the electrolyte accumulate in the negative electrode and the anions in the positive electrode, forming an EDL that compensates for the external charge disequilibrium. Conversely, in the discharge phase, electrons move from the negative electrode to the positive electrode, again through an external circuit, and the opposite types of charge combine again in the pores until the cell is completely discharged. The ions do not move in the electrolyte in the same way as they do in the pores of the electrode, in fact, their mobility in the pores is strongly influenced by the size of the pores themselves, which, if too small for the ions to pass through, do not contribute to the double-layer capacity. Not all pores are, therefore, accessible to ions and thus there is no linear relationship between the capacitance displayed by a material and its specific

surface area. In general, it has been observed that the capacitance of a supercapacitor is increased by the presence of a small amount of mesopores (thickness greater than 2nm). Traditionally, a model is used that gives the capacitance as a function of surface area in the presence of mesopores: $\frac{C}{A} = \frac{\varepsilon_r \varepsilon_0}{b \ln(\frac{b}{b-d})}$ where b is the radius of the pores and d is the distance between the surface and the ion. In the case of micropores, considering a realistic approximation of the pore shape as a slit, the capacitance as a function of surface area is given by $\frac{C}{A} = \frac{\varepsilon_r \varepsilon_0}{b - a_0}$ with a_0 effective size of the ion [14].
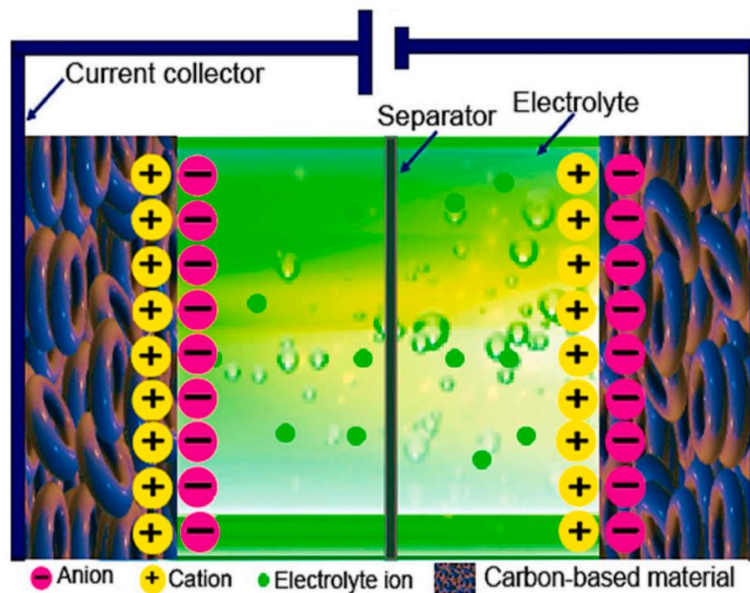
Figure 3. Scheme of an EDLC Supercapacitor [1].

1.2.2 Pseudocapacitors

The mechanism of pseudocapacitance is based on faradic charge accumulation, which can occur through redox reactions near the surface or through highly reversible fast reactions directly on the surface. As for a double layer, theoretically, the electrical response of a pseudocapacitive material is also based on a continuous change of charge state with potential, leading to a constant of proportionality that is the capacitance. Some psudocapacitors use electrodes made of conductive polymers or metal oxides and sometimes functionalised porous carbons. These materials can also store a significant charge in a double layer, thus combining capacitive and pseudocapacitive storage mechanisms. In general, a pseudocapacitive material can be intrinsic, exhibiting pseudocapacitive behaviour over a wide range of particle size and morphology, or extrinsic, in which pseudocapacitive behaviour only appears for certain conditions in the surface of the nanoscale materials and not in the bulk. Several charging mechanisms can be distinguished in a pseudocapacitive electrode: sub-potential deposition, redox reactions of transition metal oxides, pseudocapacitance by intercalation and also doping and reversible electrochemical dedoping in conductive polymers. The materials used to make these electrodes are normally carbon, metal oxides and conducting polymers [14]. These materials can achieve much higher specific capacitance values than EDLCs due to the charge storage mechanism based on fast redox reactions occurring on the electrode surface and not in the bulk as with batteries. However, as with batteries, the redox reactions can cause mechanical stresses in the electrode (swelling or shrinkage), resulting in poor mechanical stability and consequently reducing the life cycle [2,14].
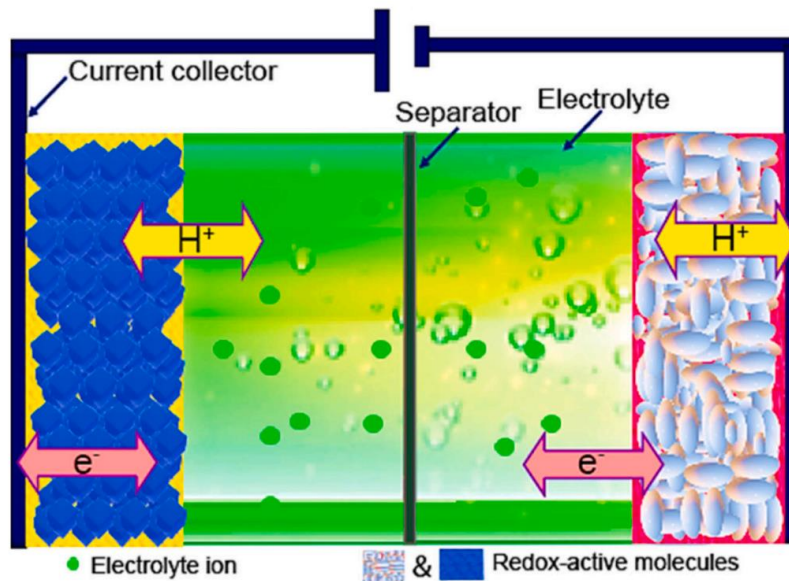
Figure 4. Scheme of an Pseudocapacitor [1].

1.2.3 Hybrid Supercapacitors

It is also possible to consider a third type of supercapacitors based on both faradic and non-faradic processes: hybrid supercapacitors. They behave on the one hand as pseudo-capacitors, overcoming the limitations of EDLs but can achieve the cyclic stability and power density typical of EDLs [1,14]. We can distinguish three types of hybrid supercapacitors depending on the materials used for the electrodes: asymmetric, battery type, composite hybrid. The first two types share similarities in terms of the arrangement of the electrodes, which are characterised by different materials. In asymmetric hybrids, for example, the negative electrode, typically made of carbonaceous materials, behaves like an EDLC; the positive electrode like a pseudocapacitor. The choice of having one electrode governed by an EDLC mechanism and the other as a pseudocapacitor is preferred because this combination provides a wider potential window, greater cyclic stability and a longer life cycle. However, it is possible for both electrodes to be made of the same material (e.g. carbonaceous materials with different functional groups inserted inside), but even in this case the structure is still considered asymmetrical. In the hybrid battery-type supercapacitor, one electrode is made as a battery and the other as a supercapacitor. This results in high power density (provided by the supercapacitor) and energy density (provided by the battery). Finally, in composite hybrids, the electrodes are similar and the material used to make them is usually carbonaceous embedded with pseudo-capacitive materials

such as conductive polymers and metal oxides. This increases the specific capacitance, corrosion stability and widens the potential window of the supercapacitor. In addition, carbon incorporated into conductive polymers increases their structural stability [1].
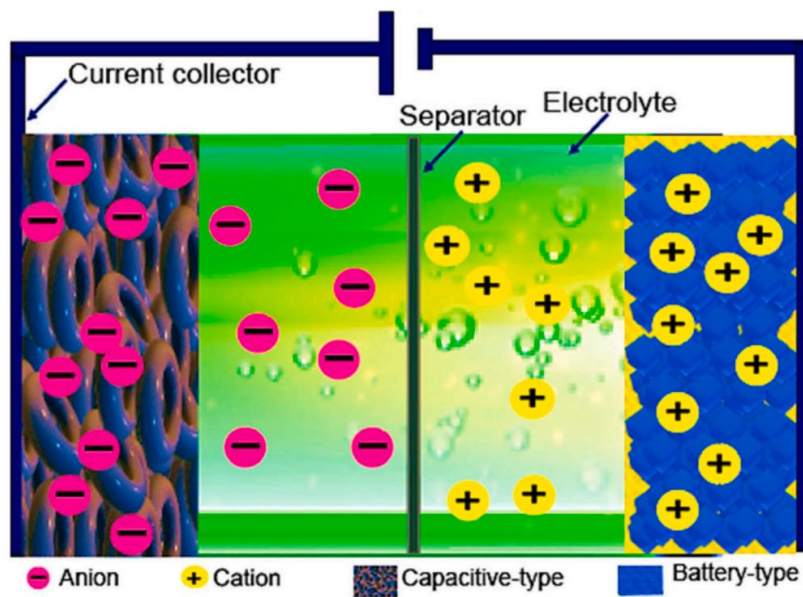
Figure. 5 Hybrid Supercapacitor [1].

CHAPTER 2:
ELECTRODES IN SUPERCAPACITORS

The most important component in a supercapacitor is the electrode. In principle, electrodes are conductors used to establish electrical contact with a non-metallic part of a circuit (in our case, the electrolyte of a supercapacitor cell). As we have mentioned, electrodes are made of nanometric materials that have a high surface area and porosity [15]. Charge is stored and separated at the interface between the solid conductive particles and the electrolyte. This interface is equivalent to a capacitor with a capacitance $C = \frac{A\varepsilon}{4\pi d}$, with A surface area of the porous electrode active material, ε dielectric constant of the electrolyte medium in which the electrodes are immersed, and d effective thickness of the double layer. In EDLCs, the material used to create the electrode is usually carbon and is not, as we have already seen, electrochemically active, i.e. no chemical reactions take place but pure physical accumulation of charge at the electrode/electrolyte interface, unlike in Pseudocapacitors. Apparently, therefore, the capacitance of a supercapacitor is strongly dependent on the surface area of the electrode. But actually, not all of the electrode's specific surface area is electrochemically accessible when the electrode is in contact with the electrolyte. The pore size of the electrode material plays a very important role: when it is close to the size of the ions in the electrolyte and there is a match between the two, maximum capacitance is obtained, while larger or smaller sizes produce a substantial decrease due to mismatch. Consequently, when studying the capacitance of an electrode, it is necessary to consider a more accurate definition of electrochemically active area, the effective area that is considered in the capacitance measurement. Optimising the porosity of the electrode to achieve high performance must therefore take into account both the size of the pores and their distribution on the surface of the active material. In conclusion, the capacitance of a supercapacitor strongly depends on the effective surface area of the electrode accessible to the electrolyte [15].

2.1   Electrodes Materials

In general, we distinguish three categories of electrode materials: conducting polymers, metal oxides and carbon materials with a high specific surface area [15].

2.1.1 Conducting Polymers

Conductive polymers are characterised by several advantages such as low cost, low environmental impact, high conductivity under doping, high potential window, high porosity, capacitance, reversibility, and redox reactions that can be tuned by chemical modification. This is why polymers are used in pseudocapacitors based on oxidation-reduction processes. During oxidation, ions are transferred to the polymer backbone; when reduction takes place, ions are released from the backbone into the electrolyte. These reactions, which are highly reversible, take place in the entire polymer bulk and not only on the surface. Conductive polymers can be positively or negatively charged by inserting ions into the polymer matrix to balance the injected charge. Electrical conductivity can therefore be modified through oxidation or reduction reactions that generate delocalised electrons on the polymer chain. Polymers that are positively charged through oxidation of repeated units of the polymer can be considered 'p-doped', while those negatively charged through reduction 'n-doped'. Supercapacitors based on conductive polymers can be of three types:

- In the symmetrical p-p type, both electrodes are made of p-type polymers. When fully charged, one electrode is in a fully doped p (positive) state and the other in an uncharged state. The potential window is 0.8-1V.In the asymmetric p-p' type, two different p-doped polymers with different electroactivity ranges of oxidation and reduction are used.
- In the symmetrical n-p type, the electrodes are made from the same polymer that can be either p- or n-doped in the same molecule. The applicable voltage is up to 3.1V in non-aqueous solution.

Conductive polymers can work in a narrow potential window beyond which they can degrade (in the case of a positive potential) or pass into an insulating state (in the case of a negative potential) [15].

2.1.2 Metal Oxides

Compared to carbon materials, metal oxides can give higher energy density, energy that is not only stored through electrostatic processes, but also through faradic electrochemical reactions between electrode and electrolyte. Compared to polymers, they also exhibit better electrochemical stability. To be used in supercapacitors, oxides must be electronically conductive, the metal may have two or more oxidation states, and protons may interact with the oxide lattice for the reduction reaction or outside the lattice in the case of oxidation [15].

2.1.3 Carbon materials

Carbon materials are considered one of the most important materials in the supercapacitive application and also in the in industry field as a fuel, to form metal alloys, as a component in paints and inks, to manufacture high-tech components in vehicles and so on. They have numerous advantages such as abundance and low cost, easy processability, non-toxicity, high specific surface area, good electrical conductivity, high chemical stability, and a wide operating temperature range. They normally store charge in an electrochemical double layer at the electrode/electrolyte interface rather than in the bulk of the material. Thus, capacity depends primarily on the surface area accessible to the ions of the electrolyte. The most important factors influencing performance are therefore surface specific area, pore size distribution, pore structure and shape, electrical conductivity and surface functionality, with greater importance given to surface specific area and pore size distribution. In general, carbon materials used in EDLCs should ideally have a high specific area (around 1000 m^2 g^{-1}), good intra- and inter-particle conductivity in the porous matrix, and good accessibility to the pore space of the carbon material. In summary, when selecting the carbon material for the supercapacitor, one must look for high and accessible specific surface area with good electrical conductivity. There are various carbon materials with a large specific surface area: activated carbon, carbon aerogels, carbon nanotubes (CNTs), templated carbons, carbon nanofibers. In general, carbon materials with a larger specific surface area have a higher charge storage capacity at the electrode/electrolyte interface. It is possible to increase the specific surface area through various techniques such as heat treatment, or alkaline treatment, activation with steam or CO_2 and plasma surface treatment with NH_3. These methods can effectively create micropores and defects on the carbon surface, resulting in an increase in specific surface area, but the specific capacity is not always directly proportional. This is because it is not certain that all the micropores on the electrode surface are accessible to the ions of the electrolyte. The optimal pore diameter for matching ions appears to be between 0.4 and 0.7nm in an aqueous electrolyte, and 0.8nm in an organic one. Another method to increase specific capacity is surface functionalisation in which functional groups or heteroatoms on the surface can increase ion adsorption in conjunction with the hydrophilicity or lipophilicity of carbon materials, producing higher wettability and faster ion transport within the micropores. In addition, the inclusion of functional groups or heteroatoms on the carbon surface can induce faradic redox reactions that increase the total capacity by 5-10 %. The most used heteroatoms are oxygen, nitrogen, boron and sulphur, but the presence of these functional groups or heteroatoms increases the risk of electrolytic decomposition, especially in the case of organic electrolyte. In addition, the presence of heteroatoms can

lead to an increase in the intrinsic electrical resistance of the material since bound heteroatoms possess a higher reactivity that produces a barrier to electron transfer. It is possible to further increase the total capacity by adding conductive polymers to the carbon material. The drawback here is that due to the rapid degradation of polymers, the device life cycle remains low (<100000 cycles). Ultimately, carbon materials with a high surface area and porous structure appear ideal for EDLC fabrication. Unfortunately, however, the high resistivity due to the contact resistance between the carbon particles generates high internal series resistance (ESR), reducing the performance of the supercapacitor. Furthermore, the surface area inaccessible to the electrolyte hinders the performance of the carbon material [15].

In this discussion, the various types of carbon-based materials in electrodes will now be analysed. I will first discuss the synthesis methods and then study the characterisations required to measure relevant physical parameters involved. Finally, simulation techniques will be introduced to study possible solutions to technological limitations.

CHAPTER 3:
CARBON-BASED ELECTRODE MATERIALS

As we have seen previously, in the choice of the charge storage mechanism governing the supercapacitor, the material from which the electrodes are manufactured plays a crucial role. Carbon-based materials are typically used in non-faradic processes (typical of EDLCs), while metal oxides, conducting polymers, and non-metal oxides are mainly used in faradic processes [1].
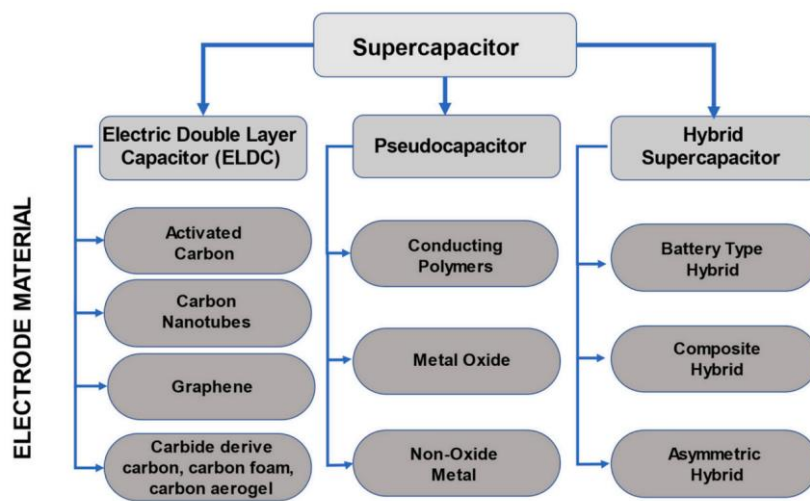
Figure 6. Classification of supercapacitor and its electrode material [1].

As seen in Figure 6, carbon is the key element in the construction of ELDC electrodes due to the simultaneous presence of chemical and physical characteristics that make it very versatile and advantageous. The main features are:

- High conductivity: high conductivity can ensure rapid electrical transport through the bulk, minimising internal resistance and facilitating charge transfer and the subsequent storage. Conductivity can be set through a certain level of doping which changes the charge density. Furthermore, in carbon-based materials, the presence of a high percentage of sp^2 hybrid orbitals contributes to the delocalisation of electrons and increased conductivity [3,4,9].

- High accessible surface-area: since the energy storage mechanism resides on the electrical double layer at the interface between electrode and electrolyte, a high surface area provides high space for charge accumulation and a corresponding increase in specific capacity and energy density. However, a high surface area results in a large number of pores, voids and channels that can trap the electrolyte and reduce charge accumulation. The pore design must therefore be carefully balanced against the morphology of the electrode [3,4,9].
- Excellent corrosion resistance [3,4,9].
- High thermal stability [3,4,9].
- Controlled pore size distribution: although, as mentioned earlier, high pore size can reduce capacitance, a correct pore size in the electrodes is crucial for proper wettability and surface accessibility of ions. Pores less than 2 nm in diameter (micropores) increase the surface area of the electrodes and contribute to charge storage, while pores between 2 and 50 nm in diameter (mesopores) provide interconnecting channels for rapid ion transport. Pores with a diameter greater than 50 nm (macropores) can act as an ion reservoir to attenuate the abrupt change in electrolyte concentration when high current density is present. Conversely, macropores tend to absorb an extra concentration of electrolyte in the channels, leading to an increase in electrode weight. Careful control of the pore distribution is therefore necessary to obtain the best possible compromise that maximises advantages while minimising drawbacks [3,4,9].
- Long-term electrochemical stability: carbon materials are generally electrochemically stable because the charge separation in the double layer at the electrode/electrolyte interface, inherent to the storage mechanism of EDLCs, does not induce chemical reactions. However, impurities in the electrode can react with the ions due to catalytic decomposition, leading to irreversible parasitic reactions that decompose the electrolyte, thereby decreasing capacitance [3,4,9] .
- Satisfactory compatibility in composite materials [3,4,9].
- Low cost [3,4,9].

In this thesis work, we will focus precisely on carbon-based electrodes, analysing their structures, properties and parameters that impact performance. We will examine both experimental data and numerical simulations.

3.1 Synthesis and characterisation

3.1.1 Templated Carbon

The procedure for synthesising templated carbon consists of infiltrating a carbon precursor into the pores of a template; a carbonisation treatment is then performed and, finally, the template itself is removed to obtain a well-ordered nanoporous carbon structure with a well-controlled pore size distribution, a large specific surface area and an interconnected pore network [2].
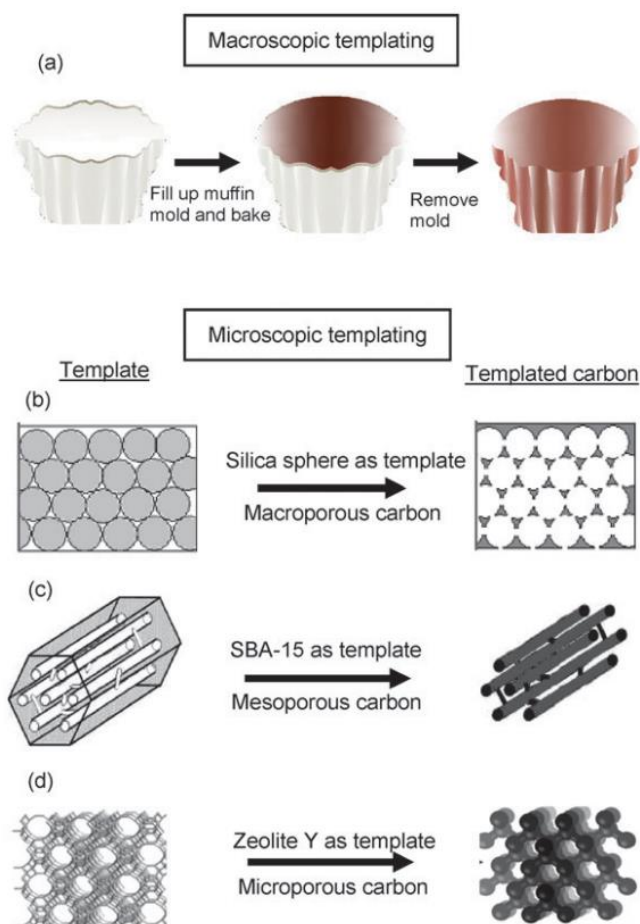
Figure 7. (a) Macroscopic representation showing the general concept of the templating technique; microscopic synthesis of (b) macroporous carbons using silica spheres as template, (c) mesoporous carbons using SBA-15 as template and (d) microporous carbons using zeolite Y as template [2].

Compared to Activated Carbons (see section 3.1.5, page 30), whose micropores are basically disordered and have a broad size distribution, templated microporous carbons have a narrow pore size distribution optimised with respect to the size of the ions in the electrolyte. Furthermore they are characterized by ordered straight pore channels that are excellent for use as materials for high-energy-density electrodes. In addition, a well-controlled pore structure facilitated the use of pseudo-capacities from nitrogen and oxygen functional groups of carbon materials. The presence of mesopores (2-8 nm) can accelerate ionic diffusion in electrodes and increase power performance at high current densities, while micropores accessible to electrolyte ions are crucial for high energy storage. Based on these considerations, it is possible to realise a hierarchical porous graphitic carbon (HPGC) material, a three-dimensional structure with macroporous cores (acting as ion-buffering reservoirs), mesoporous graphitic walls (providing excellent electrical conductivity, capable of overcoming the limitations of electrochemical processes in porous electrodes) and micropores (increasing stored energy) for applications in high-performance supercapacitors [2].
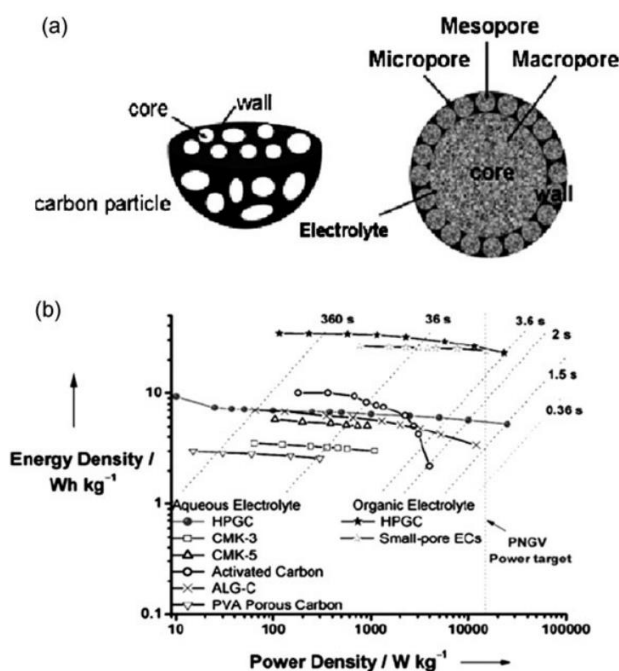
Figure 8. (a) Schematic representation of the 3D hierarchical porous structure (HPGC) and (b) Ragone plot comparing the performance of HPGC material with those of CMK-3, CMK-5, activated carbon (Maxsob, Japan), ALG-C, PVA porous carbon, and small-pore EC. The dotted lines show the current drain time [2].

The template method thus proves to be one of the best techniques for controlling the porosity of materials, and by carefully selecting the template materials, carbon precursors and carbonisation processes, it is possible to obtain nanoporous carbon templates with desired physical and chemical properties. At the expense of their high cost, carbon templates are promising structures for future electronic applications [2].

3.1.2 Carbride-Derived Carbons (CDCs)

Carbide-derived carbons (CDCs) are carbonaceous materials that could increase the power density (around 200kW/Kg) and potential window (up to 3.1V) of supercapacitors. CDCs are synthesised by means of the sol-gel process (method to prepare a material based on the preliminary formation of a colloidal solution, which then evolves to form a gel, which is then dried to produce the final material) or by etching with chlorine (Cl2) specific metal carbides such as silicon carbide (SiC), boron carbide (B4C), titanium carbide (TiC). The latter is the most widely used because it provides the most significant amount of stored charge density with subnanometer pore size. The properties of CDCs are influenced not only by the materials used, but also by the synthesis methods. For example, the etching process can change the pore size distribution, while the sol-gel process can produce a more uniform crystal structure [1].
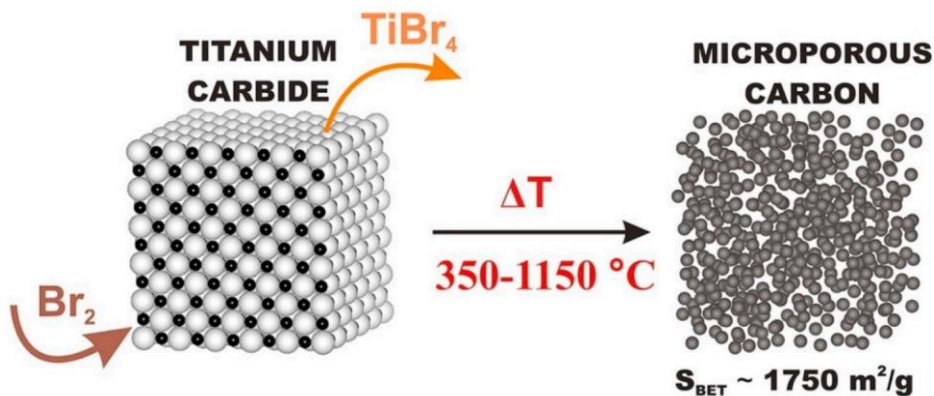
Figure 9. Graphical illustration of the preparation of CDC from bromination of TiC [1].
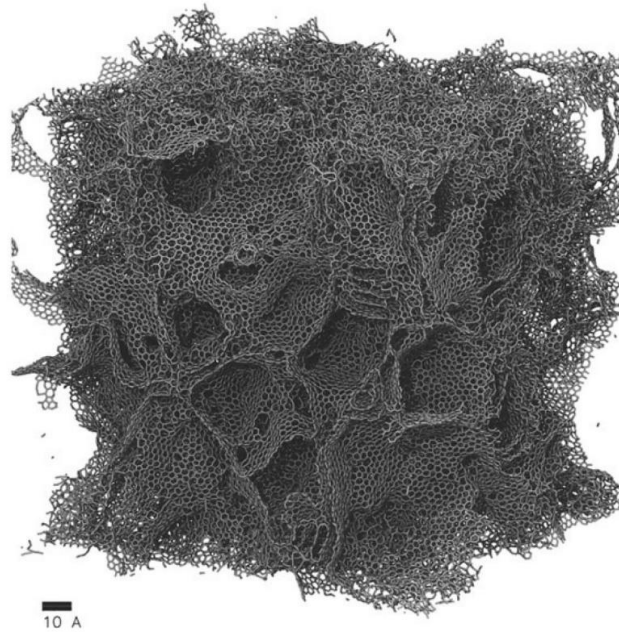
Figure 10. Structure of a general model of CDC [1].
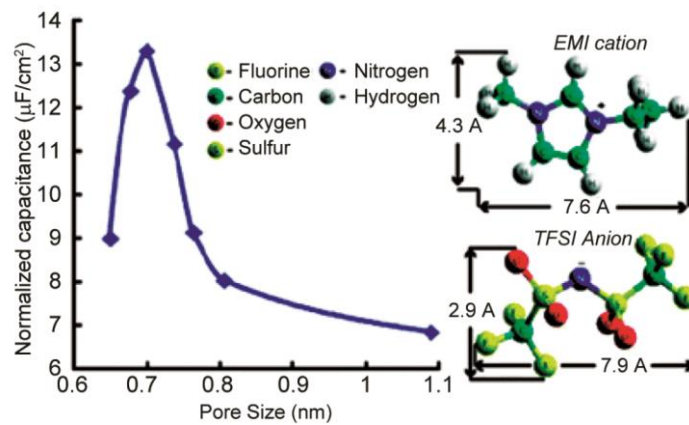
Figure 11. Variation of capacitance as a function of pore size for CDC samples in the presence of Ionic liquid (EMI–TFSI) based electrolyte [1].

3.1.3 Graphene

Graphene is a single layer of sp^2-hybridised carbon atoms forming a honeycomb structure that possesses exceptional mechanical properties, superior even to those of steel, such as a tensile strength of up to 128 GPa, although the thickness of the graphene structure is only that of a carbon atom. It also has excellent electrical conductivity (6.6×104 S/m) and thermal conductivity (5450 W mK^{-1}), large surface area (3269 m^2/g), good chemical stability (400 mJ cm^{-2}) and excellent flexibility with an elastic modulus of 1.3TPa, making it the most promising material for future generations of electronic devices. The main drawback of using grapheme, however, is the ease with which the atoms in the structure can rearrange and aggregate, leading to a breakdown in symmetry, resulting in a decrease in intrinsic and total capacitance. Thus, the capacitive efficiency of a supercapacitor using graphene decreases over time. As a solution, graphene layers are either modified to produce 2D or 3D structures or doped with heteroatoms such as oxygen to increase porosity and specific capacitance (graphene oxide). In the latter case, oxygen counteracts the formation of agglomerates in the graphene lattice during synthesis and utilisation, increasing the superconducting capacity [1].
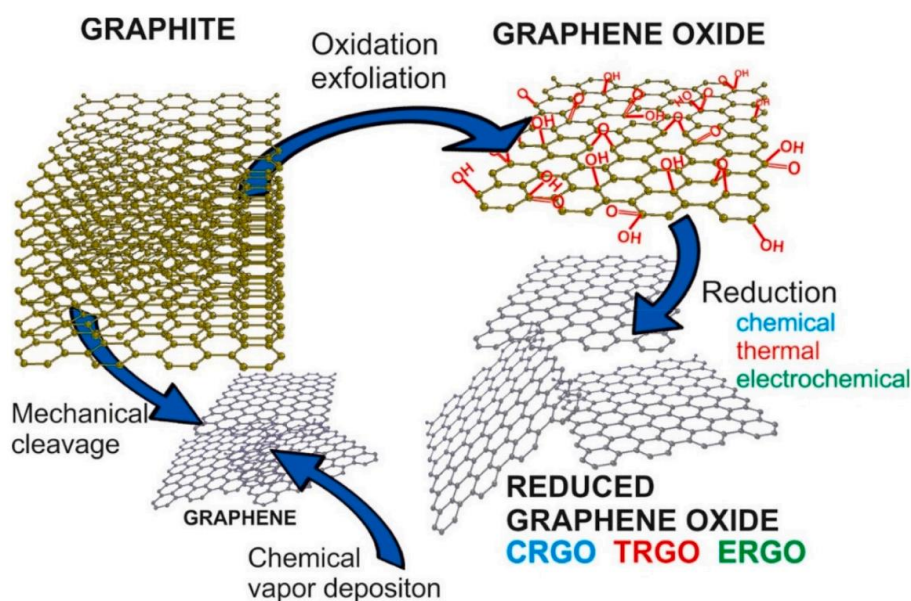
Figure 12. Graphical representation of the lattice structure of graphene, graphene oxide and reduced graphene oxide [1].

The use of graphene oxide increases the specific capacity of supercapacitors by 500 times and also increases power density. It is also possible to incorporate graphene oxide/reduced graphene oxide with transition metal carbides/nitrides (MXene), conductive polymers, metals, metal oxide/hydroxide/sulfide in order to further improve the electrochemical properties of electrodes. Combining MXene with graphene oxide can also increase the flexibility of electrodes, with extensibility increasing by up to 300%. Graphene is also used in research to make graphene-based quantum dots (GQDs). Graphene-based quantum dots are found to have higher electron transfer than those based on generic carbon, increasing the conductivity of the electrode [1].
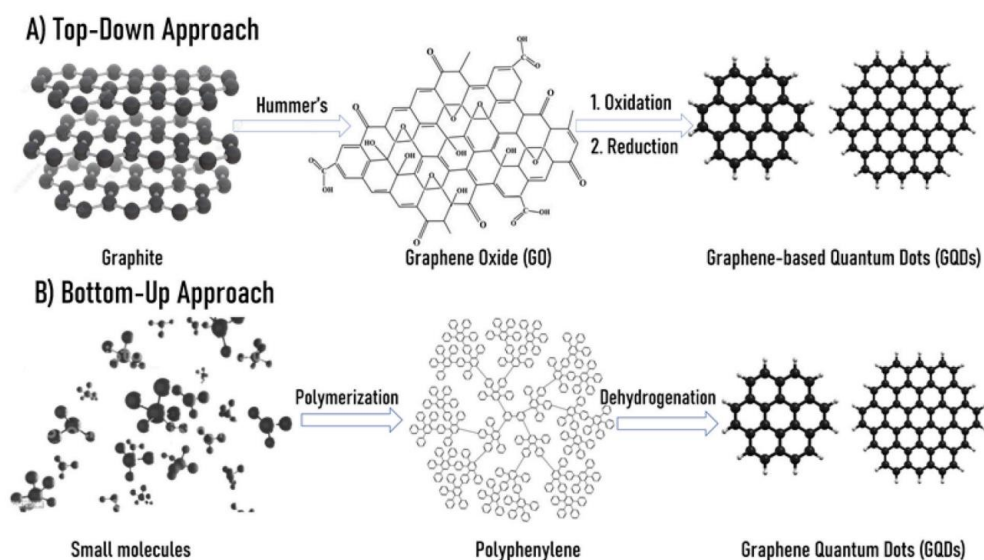
Figure 13. Graphical outline of top-up and bottom-up preparation method of GQDs [1].

By combining graphene (sp^2-hybridised carbon) with linear acetylene (sp-hybridised carbon), it is possible to make a hybrid form called graphdiyne that enhances its chemical activity and physical stability and possesses exceptional processability and controllability characteristics that together contribute to superhydrophobicity when incorporated on substrates with contact angles up to 148°. Furthermore, graphdiyne gives rise to quantum capacitance with modifiable electronic properties when doped with boron or nitrogen induces semiconductor-to-metal transitions. In these cases, high capacitance values in the electrodes of 4317 F/g (in the case of boron doping) and 6150 F/g (for nitrogen doping) can be achieved [1].

3.1.4 Carbon Nanotubes (CNTs)

Carbon nanotubes are tubular structures obtained by concentric cylindrical winding of individual layers of graphene. They have excellent mechanical properties, good thermal stability and a unique porous structure as they are characterised by nanofibres with highly interconnected mesopores that allow interaction with a wide range of ionic quantities, leading to a large specific surface area that consequently produces peaks in conductivity. The high conductivity values are also achieved due to the ballistic transport that ions undergo within the structure of CNTs, where the high free mean path of ions before scattering events produces a lowering of resistance. This contributes to increased power density when used in supercapacitors [1]. It is possible to distinguish between two types of CNTs:

- Single-walled carbon-nanotubes (SWCNT) in which nanoscale graphene sheets are rolled into a cylindrical shape and closed at the end of the tube with half a fullerene molecule.

- The multi-walled carbon-nanotubes (MWCNT) in which we have single nanotubes concentrically distributed inside each other.
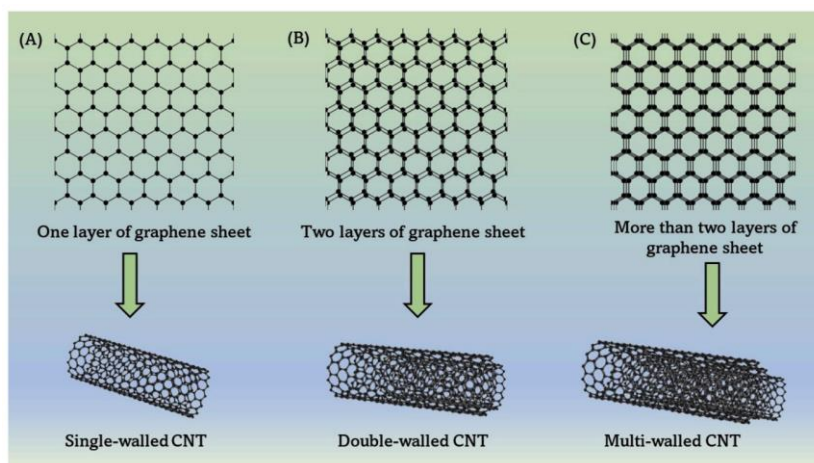
Figure 14. Types of CNTs; Single-walled Carbon Nanotube (SWCNT), Double-walled Carbon Nanotube (DWCNT) and Multi-walled Carbon Nanotube (MWCNT) [1].

Although a multi-walled carbon-nanotube has a larger surface area, the presence of structural defects within each winding makes single-walled carbon-nanotubes superior in terms of specific capacity. Oxygen doping, polymers, metal oxides and

metal sulphides can be used to increase the specific capacitance and overall electrochemical performance of single nanotubes. For example, the use of a nitrogen-doped CNT with Co-Co_3O_4 particles inside as the electrode material of a supercapacitor has led to excellent specific capacitance (823.4 F/g) and power density (1601.1 W/kg) values with a stability of 93.6% over 10000 cycles. It is also possible to combine CNTs with transition metal carbides/nitrides (MXene), thus promoting ion transport and increasing capacitance to 300 F/g values with 92% retention capacity even after 10000 charge/discharge cycles at 20 A/g. The excellent mechanical properties of CNTs have led to the realisation of flexible solid-state supercapacitors using ternary fibres formed from CNTs, CNTs and polyaniline (PANI) fibres, or by adding a self-healing material, stretchable carboxylate polyurethane (PU) on the CNT/Graphene/PANI composite film. Although CNTs have excellent properties, the limited useful surface area and the difficulty in purification processes as well as the high production cost still severely limit their use in supercapacitors [1,2].

3.1.5 Activated Carbons (ACs)

Activated carbons (ACs) are amorphous carbon structures that, through an activation process, have porous structures that increase their surface area available for adsorption or chemical reactions. They are, indeed, the most commonly used materials for electrodes due to their large surface area (even greater than 1000 m^2g^{-1}), pore volume (greater than 0.5 cm^3g^{-1}), good electrical properties and low cost, especially compared to graphene [2,5,11]. The process of making ACs is significantly cheaper and simpler than for other carbon materials [16]. Activated carbons can be produced by carbonisation and activation. Carbonisation is the process that converts organic matter into carbon, while activation is the process that creates the porous structure [16.] Activation can be physical (thermal) or chemical of various carbonaceous materials that can be found in various forms such as fibers, pellets, cloths or felts [11]. Physical activation refers to a two-step process, with pyrolysis, of carbon precursors (wood, coal, nutshell, etc.) in an inert atmosphere (usually nitrogen), in a high temperature range between 700 and 1200 °C, followed by gasification with oxidising gases such as steam, air, CO_2 or mixtures of them [2,11]. This second step is used to maximise porosity, especially when steam is used as the reduced size of water molecules facilitates diffusion into the porous carbon structure and steam activation has a faster conversion rate than CO_2 [16].Chemical activation, on the other hand, is a single-step process at a low temperature (between 400 and 700 °C), in which activating chemical agents such as phosphoric acid or potassium hydroxide KOH [2, 10], are incorporated

into carbon precursors by pyrolysis. There is also the possibility of combining the two techniques, although there are more effective methods for controlling pore size such as the template method, but at a higher cost and complexity [10,11]).

The carbon precursors used in carbonisation processes can be among the most various. One of the greatest advantages of ACs is precisely the use of waste material to make the electrodes that will later be used in supercapacitors. In the following, some examples of synthesis processes will be given.

A first type of precursor is waste tea leaves (WTL), which are dried and boiled in water. They are then pyrolysed at 600 °C for two hours under a flow of Argon to obtain the carbonaceous product. This is followed by chemical activation using KOH solution followed by evaporation at 80 °C in vacuum. The dried carbon thus produced is then heated to 800°C for one hour in an Argon atmosphere and further neutralised using 1 M HCl solution. The maximum specific capacity achieved by an electrode made from activated carbon produced from tea leaf waste was 330 F/g at 1 A/g [16].
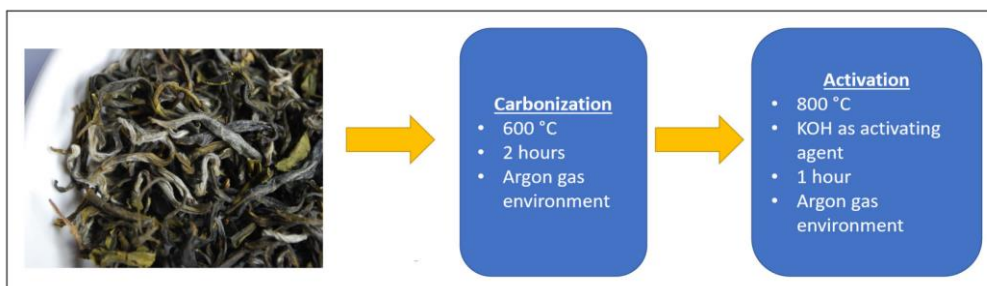
Figure 15. Two-step synthesis of activated carbon from waste tea leaves [16].

Another type of precursor is Albizzia flowers (AF), which are first dried at 600°C at a rate of 3°C per minute for three hours in an Argon atmosphere. Next, the activation process uses KOH at a temperature of 700 to 900°C at a rate of 5°C per minute. The activated samples are then treated with 1 M HCL and deionised water until a pH of 7 is reached and finally dried at 80°C for 10 h. The electrode thus fabricated achieves capacities of 406 F/g at 0.5 A/g in a 6M KOH electrolyte [16].
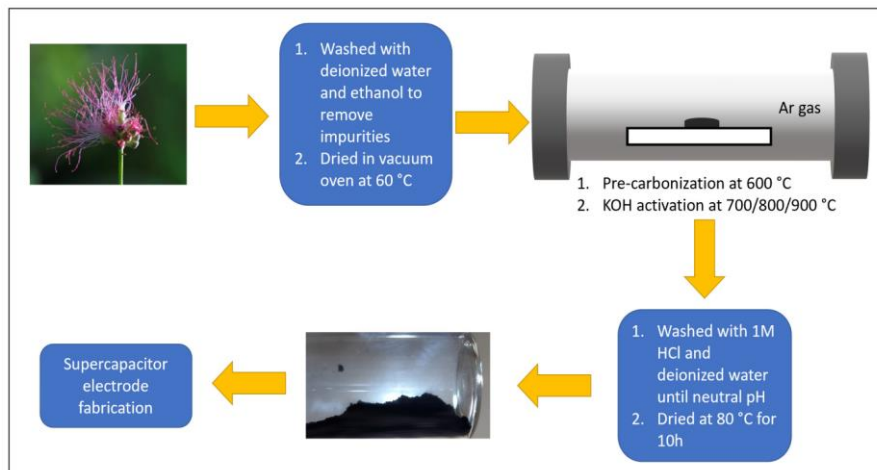
Figure 16. Process of preparing activated carbon from Albizzia flowers [16].

Using palm kernel shells (PKS) as precursors, chemical activation via KOH or physical activation via steam can be applied. The PKS are first pyrolysed in a furnace for 4 hours at 500°C in an oxygen-deficient environment. The precursors thus treated are either mixed with KOH at a rate of 1:4 for four hours at 100°C (chemically activated carbons AC-C) or activated via steam (physically activated carbons AC-P). In both cases, there is then a heating phase in a furnace at 500°C for four hours and a washing phase in 1M HCl and then distilled water until a neutral pH is reached. Supercapacitors using this type of activated carbon can reach capacities of 210 F/g (AC-C) and 123 F/g (AC-P) at 0.5A/g in 1M KOH [16].

Besides the two-step synthesis process, characterised by carbonisation followed by activation, there is also a one-step process where carbonisation and activation are carried out simultaneously. Using coffee waste as a precursor, it is mixed for 6 hours in 1M KOH. The resulting powder is washed with deionised water and then dried in a vacuum oven. The dried powder is then dispersed in an aqueous solution containing activating agents and stirred for 15 minutes. The resulting solution is then filtered and the resulting powder is finally annealed at 700°C in nitrogen for two hours. Electrodes based on activated carbon from coffee remains have a low specific capacity of 19.28 F/g but, on the other hand, the highest energy density (6.94 Wh/kg) and power density (350 W/kg) [16].
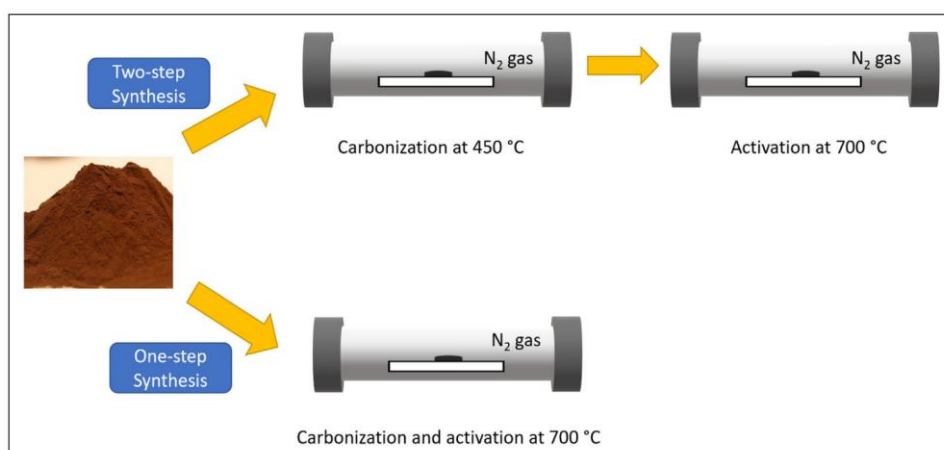
Figure 17. The process of one-step and two-step synthesis of activated carbon [16].

Another precursor that has been used to create activated carbon is the seed shells of the ginkgo plant, resulting in ginkgo-based activated carbon (GGAC). First, the ginkgo shells are dried at 60°C for 24 hours and then pyrolysed in a furnace in a nitrogen atmosphere at 600°C at a rate of 10 degrees per minute. Finally, the shells thus treated are mixed with KOH at a rate of 1:2 and heated in a nitrogen atmosphere for one hour at 700°C. The carbons are then neutralised with hydrochloric acid and rinsed repeatedly using deionised water until a neutral pH is reached. A capacity of 178F/g can be achieved with GGACs. [16].

Paulownia is a popular flower in China and used in the pharmaceutical industry. The large quantity of the waste material can be used to make activated carbon. After a two-hour pyrolysis step at 600 °C in a nitrogen atmosphere, the charred Paulownia flowers (PCF) are activated by mixing them with potassium hydroxide. The mixture is then further pyrolysed at 800 °C in a nitrogen atmosphere for one hour. The activated Paulownia is washed with 1M HCl and deionised water until a neutral pH is obtained. In the manufacture of the electrodes, the activated carbon thus obtained is mixed with active materials such as acetylene black, and polytetrafluoroethylene binder in the percentages of 85mw%, 10mw%, and 5mw% respectively. These electrodes are then separated by a cellulose hydrophilic separator and immersed in a 1M H_2SO_4 electrolyte. Such a symmetric supercapacitor results in a capacitance of 297 F/g at a current density of 1 A/g within a potential window of 2-3 V [16].

Pistachio shells can also be used to obtain activated carbon by activation at different mass rates with KOH as the activating agent and pyrolysis step at 750 °C. The samples are named AC-SPN-X where X represents the rate between

potassium hydroxide and charred shell (C-SPN). The carbonised shell shows a lamellar structure similar to that of the untreated shell but with a narrowing of the pores. AC-SPN-3 has pores with a diameter of 0.5-1nm. All carbonic samples exhibit defective graphitic structures whose degree of graphitisation depends on the ratio of the I_G/I_D currents, which increasing, leads to a higher electrical conductivity. The AC-SPN-3 sample has the highest capacitance and its CV curve shows us an almost rectangular shape [16].
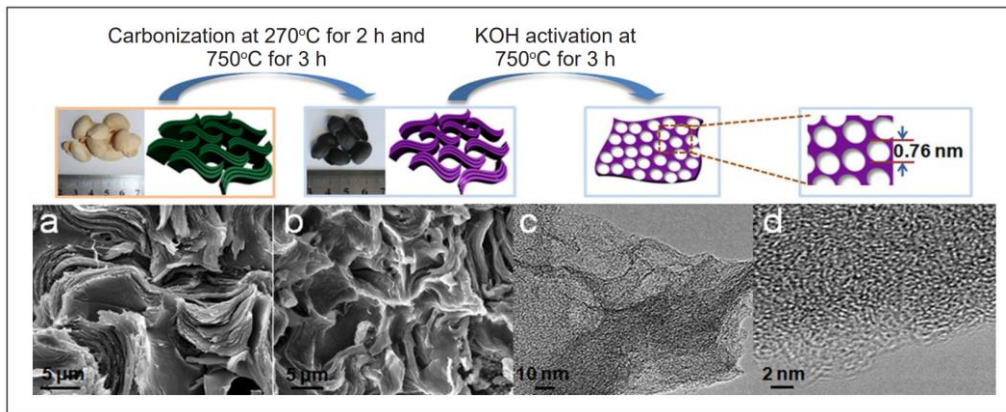
Figure 18. Process of synthesizing AC from pistachio nutshell with a) SEM of natural pistachio shell, b) SEM of C-SPN, c) and d) HRTEM of AC-SPN-3 at different magnification [16].
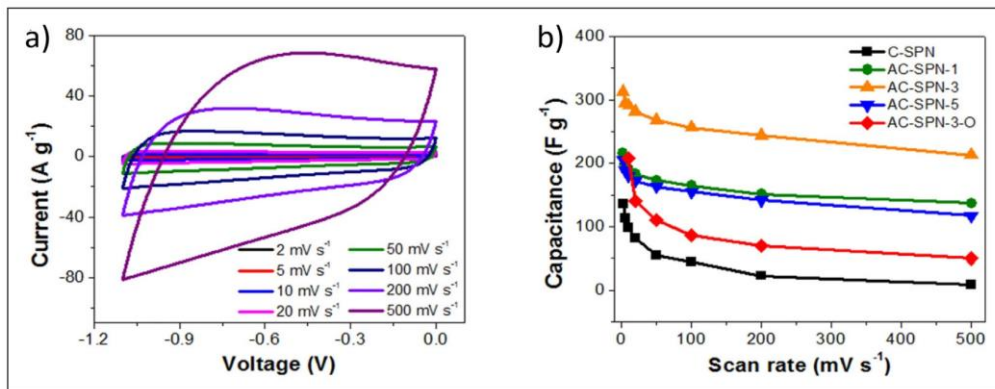
Figure 19. a) CV curve of AC-SPN-3 and b) Specific capacitance of all samples at different scan rates [16].

It is possible to obtain activated carbons from banana fibres, which are first washed and dried. They are then treated with KOH or ZnCl2 at 110 °C for 5 days and pyrolysed for one hour at 800 °C with a heating rate of 10 °C per minute in a nitrogen atmosphere. The activated carbon obtained is mixed with 20 wt% of carbon black and 5 wt% polyvinylidene fluoride, using N-Methyl-2-pyrrolidone (NMP) as a solvent to form a slurry that is then spread on a nickel mesh. After drying for 30 minutes at 110°C, the mesh is pressed to fully adhere the active electrode material to the Ni mesh. The activated carbons thus produced show a capacity of 74 F/g with a current density of 0.5 A/g and a surface area of 1097 m2/g in 1 M Na_2SO_4 as electrolyte in the case of activation with $ZnCl_2$ or 66 F/g capacity and 686 m2/g surface area when activation is performed using KOH [16].

As we have seen, there are vast possibilities in the choice of precursors for the realisation of activated carbon. The following figure shows a comparison of capacity and specific area for various types of biomass.

Biomass precursor	Activation method	S_{BET} (m^2g^{-1})	C_{sp} (Fg^{-1})
Firewood	KOH	2821	95
Coffee bean waste	$ZnCl_2$	1019	368
Cherry stones	KOH	1624	174
Coffee shell	$ZnCl_2$	842	156
Recycled wastepaper	KOH	417	180
Cassava peel waste	$KOH + CO_2$	1352	153
Sugar cane bagasse	$ZnCl_2$	1788	300
Apricot shell	NaOH	2335	348
Coffee endocarp	CO_2	709	176
Sunflower seed shell	KOH	2509	311
Rubber wood sawdust	CO_2	912	138
Argan seed shell	KOH	2062	355
Camellia olleifera shell	$ZnCl_2$	1935	374
Poplar wood	HNO_3	416	234
Fibers of palm oil empty fruit bunches	$KOH + CO_2$	1704	149

Table 3. Comparison of specific capacitance between other precursors [16].

The comparison of the characterisations of activated carbons from banana stems and those obtained from maize cobs and starch potatoes is significant. By Raman spectroscopy, partial graphitisation is observed in all cases, but the banana stem activated with KOH (KHC) shows a more disordered structure. This is an advantage for energy storage because it increases the active surface area. An

observation by scanning electron microscopy (SEM) of KHC, phosphoric acid-treated banana stem (PHC) and carbon derived from maize cob (CHC) show a greater porous structure than carbon derived from potato starch, which show no signs of porosity [16].
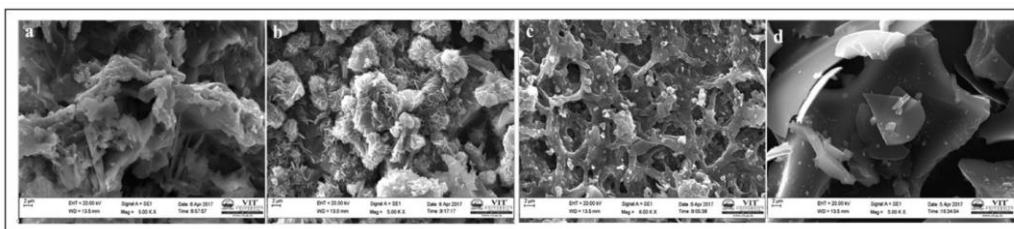
Figure 20. FE-SEM images of (a) KHC, (b) PHC, (c) CHC and (d) SHC [16]

When the carbonisation temperature was increased, more microcrystalline pores were obtained in various carbon layers, which, together with the mesopores, facilitate the transfer of charge into the carbon, thereby increasing the capacitive performance of the electrode. Comparing the four different samples data in table 4, it can be seen that a smaller pore diameter, with a consequent increase in pore volume, produces an increase in surface area and corresponding capacitance. The optimal diameter in the literature appears to be around 1 nm [16].

Sample	Specific Capacitance (F/g)	BET Surface area (m²/g)	Average pore diameter (nm)	Average pore volume (cc/gm)
KHC	479.23 @1mV/s	567.36	1.205	0.175
CHC	309.81 @2mV/s	215.42	1.199	0.107
PHC	202.11 @2mV/s	177.72	1.789	0.091
SHC	99.9 @2mV/s	42.43	1.363	0.099

Table 4. Capacity comparison table as a function of porosity [16].

Analysing the samples in the 1M KOH electrolyte by means of the voltage/current curve, an almost rectangular pattern typical of EDLCs can be observed, caused by the hydrophilic nature of the micro-ordered sheets with oxygen on the edges of the structures. In addition, redox peaks can be seen (especially for the KHC sample) indicating faradic reactions related to pseudo-capacities during charge/discharge [16]
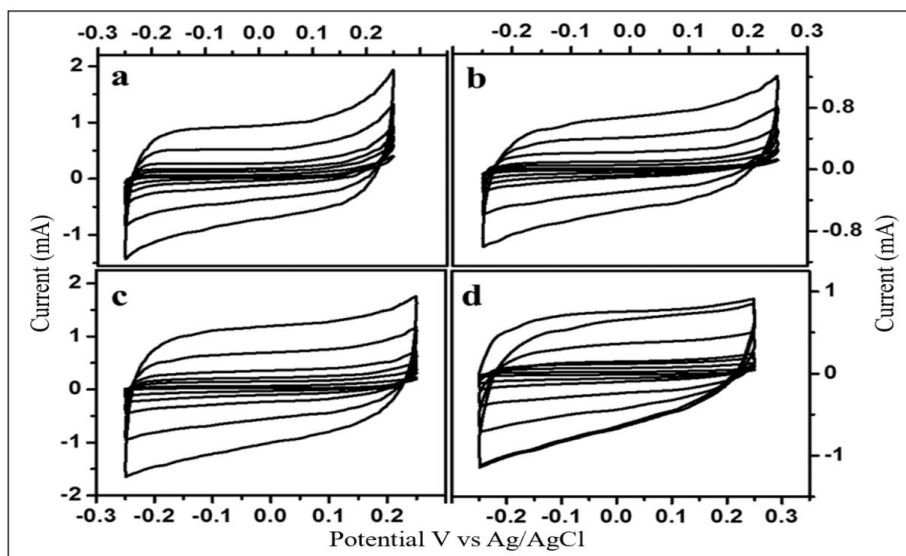
Figure 21. CV curves of (a) KHC, (b) PHC, (c) CHC and (d) SHC [16].

As we have seen, by varying the parameters of the activation processes (temperature, time, type of activating agent [10]), pores are produced in the structure of ACs with a wide distribution of their diameter ranging from micropores (diameter less than 2 nm), to mesopores (diameter between 2 and 50 nm) and macropores (diameter greater than 50 nm) [2]. Higher activation times and temperatures correspond to higher porosity. Table 5 shows how chemical activation by KOH efficiently develops micropores and, depending on different precursors and activation conditions, results in a distribution of different pore sizes as well as large surface area (approx. 4000 m^2g^{-1}) and large pore volume (up to 2.7 cm^3g^{-1}) [10,11]. Analysing, for example, the high capacitance values of the A-PM sample in table 5, they probably originate from the good electrical conductivity associated with the precursor and that the pore size comes from the intercalation of potassium during the activation process. Furthermore, the microtextural/structural order of the activated carbon may influence the electrochemical performance. All these contributions explain why a capacitance range of 7 to 11 μF cm^{-2} is observed even for materials obtained under identical conditions [10].

Sample	$S_{BET}/$ $m^2\,g^{-1}$	$V_{DR}/$ $cm^3\,g^{-1}$	Capacitance/ $F\,g^{-1}$	Specific capacitance/ $\mu F\,cm^{-2}$
A-C	3150	0.951	312	9.9
A-CS	3190	0.936	223	7.0
A-PM	2660	0.839	294	11.0
A-PS	2750	0.859	261	9.5
A-AC	1900	0.609	198	10.4

Table 5. Porosity parameters of KOH activated carbons prepared from various precursors and their capacitance values estimated by galvanostatic discharge in 1 mol L^{-1} H2SO4 solution. The precursors are coal, coal semi-coke, pitch mesophase, pitch semi-coke and a commercial activated carbon for A-C, A-CS, A-PM, A-PS, A-AC, respectively [10].

In principle, the more microporous a structure is, the greater will be its specific surface area (SSA) and thus the more surface area available for charge accumulation, which would lead to an increase in capacitance. The porous structure allows ACs to achieve a high surface area of up to 3000 m^{2}g^{-1} but this does not correspond to an equally theoretical linear increase in specific capacitance. Pore size and pore size distribution (PSD) is therefore one of the first parameters to be analysed when studying electrode performance.
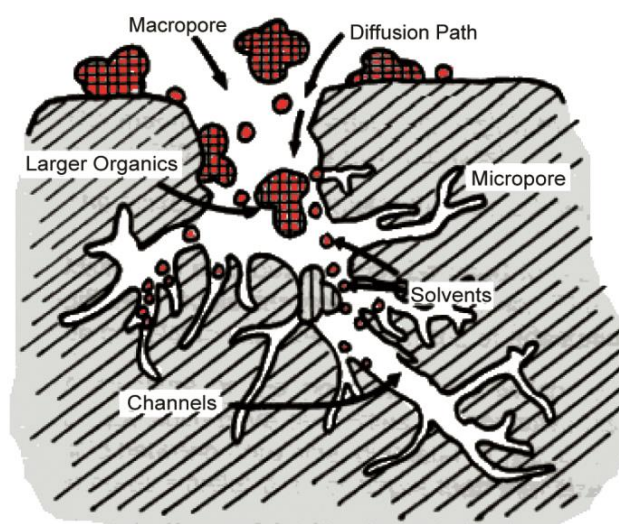
Figure 22. Schematic representation of different types of pores in Activated carbon [17].

One possible answer to this discrepancy is the fact that pores of different diameters do not all contribute to the capacitance in the same way, due to the mismatch between the ion size of the electrolyte in which the electrodes will be immersed and the pore size [2,5]. Consequently, precisely handling the size and distribution of the pores to match as closely as possible with the size of the electrolyte ions plays a crucial role in the creation of the electrodes.

To further investigate the relationship between pore structure and specific capacitance, interesting is the role of pore surface area in EDL capacitance in carbon spheres oxidised in non-aqueous electrolytes [6]. These spheres represent a special case of activated carbon characterised, as previously seen for this type of carbon structure, by an amorphous nanostructure [6]. They are prepared from resol-type phenol resin through a carbonisation process at 1000 °C [6]. Then, were oxidized at various temperatures from 380 to 500 °C for various periods in a flow of air, which was dried by passing through the silica gel column at a rate of about 50 ml/min. Spheres oxidised give rise to a wide range of pore structures. What is noticeable is that the capacitance contribution of mesopores is 10 times greater than that of micropores. This result is taken up and used as a strategy to find a compromise between the greater surface area of the micropores and the greater capacitance given by the matching of ions with the pores themselves. To do this, asymmetric capacitors are used in which the electrodes have a different pore size distribution, considering the different radii of the cations and anions [10]. In particular, the negative carbon electrode with a higher proportion of mesopores than the positive one is used. In this way, the micropores provide a high surface area and the mesopores a high performance rate [7]. Table 6 shows some capacitance and internal resistance values in capacitors made from two different type of activated carbon, obtained using tetraethylammonium tetrafluoroborate, $(C_2H_5)_4N^+ BF_4^-$ in acetonitrile, as a function of pore size [10].

	Negative electrode	Positive electrode	Volumetric capacity/ $F\ cm^{-3}$	Internal resistance/ $m\Omega$
Capacitor 1	A	B	26.6	24
Capacitor 2	A	A	20.8	23
Capacitor 3	B	B	27.5	257
Capacitor 4	B	A	18.8	243

Table 6. Effect of the pore size on the volumetric capacitance and the internal resistance of capacitors made from two carbons A and B. The pores of carbon B are smaller (an average pore diameter of 1.2 nm) than those of carbon A (1.6 nm) [10].

As can be seen from the data, the asymmetrical configuration with a larger pore diameter in the negative electrode maximises capacitance and minimises internal resistance. One of the main objectives emerging from these results is to find the right ratio between micropores and mesopores and their thicknesses to maximise the positive effects on capacitance. This goes hand in hand with the choice of electrolyte. For example, the relationship between nanopore size and an electrolyte is analysed using a model that mimics an asymmetric ionic liquid mixture containing tetrafluoroborate BF_4^- , bis(trifluoromethylsulfonyl)imide ($TFSI^-$), and 1-ethyl-3- methylimidazolium ($EMIm^+$). Three ionic systems are considered in which the molar concentration (x) of $BF4^-$ is varied (Figure 23) [8].
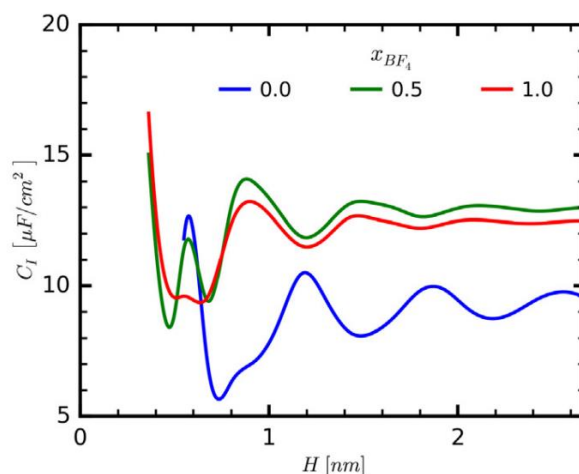
Figure 23. Integral capacitance versus the pore size for a neat symmetric (x = 0.0) and a neat asymmetric (x = 1.0) ionic liquid and for their equal molar mixture (x = 0.5). In all cases, the surface potential is fixed at 1 V [8].

Looking at Figure 23, it can be seen that, above 0.6 nm pore thickness, the capacitance in systems with asymmetric ionic liquids is significantly higher, so an increase in pore size is preferable. It is therefore clear that, by appropriately modifying the ionic mixture, the capacity of the double layer can be maximised [8]. In conclusion, the micropores are necessary for ionic absorption leading to high capacitance, while the mesopores allow rapid charge transport to the bulk of the material. Generally it is indicated that optimal performance would be achieved with pores smaller than 1nm well balanced by mesopores [10].

In addition to the impact of pores, it has been observed that high capacitance values in activated carbons via KOH can be linked to surface wettability (action

that changes the surface of a nanomaterial) [10]. In particular, it has been noted that the large amount of oxygen groups (e.g. obtained by activation at 700 °C) can lead to increased wettability on the surface of the carbon or contribute to additional pseudocapacitance, especially on the negative electrode. Unfortunately, it appears that the high concentration of oxygenated acid functional groups on the carbon can severely diminish the life cycle of the devices [10].

CHAPTER 4: SIMULATIONS IN CARBON ELECTRODES

As discussed in previous chapters, porous structures are essential in supercapacitive applications, especially nanoporous carbon structures. In nature, however, these structures are essentially disordered, and therefore, unlike crystalline materials that exhibit long-range order and for which accurate structural information can be obtained through X-ray diffraction, experimental techniques can only give limited information. Thereby, a molecular model of nanoporous carbon cannot be obtained only through experimental data and simulations plays a fundamental role to achieve e more complete understanding on these systems [18].

The techniques for creating models of nanoporous structures could be divided into three macro-categories [18]:

- The Construction method in which the porous structure is recreated through the aggregation of basic building blocks. Of course, the choice of basic blocks and the algorithm used to bind them together is not trivial and requires a detailed knowledge of the chemistry of the system [18].

- The Reconstruction method, an optimisation technique to minimise the differences between experimental data and the atomistic model for various structural characteristics. The most popular algorithm used in this method is Reverse Monte Carlo (RMC), which usually takes empirical force fields into account in order to obtain results close to the experimental data. By combining the Reverse Monte Carlo method with the Metropolis Monte Carlo, a hybrid reverse Monte Carlo method (HRMC) can be obtained that employs an accurate bond-order carbon potential. The model thus turns out to have correct chemistry, density and structure but the accuracy is highly dependent on the experimental inputs. For example, X-ray diffraction (XRD) or small-angle scattering (SAXS) provide mainly short-range structure data and, therefore, the HRMC algorithm using radial distribution functions (RDFs) from XRD is more suitable for studying micropores than mesopores. Finally, using the HRMC, the final structure is very dependent on the choice of initial structure [18].

- The mimetic approach simulates the effective synthesis processes of the porous sample. It is the most physically reliable model but also the most difficult to generate as the complexity of reactants, reaction mechanisms and experimental procedures are too complex for current computational capabilities. Therefore, the

mimetic approach has usually been used on models with extremely simplified synthesis processes [18].

From the perspective of studying carbon structures at the nanoscale, Molecular Dynamics (MD) is the most effective method for studying the interactions between particles and reproducing their behaviour [12]. Starting from numerical solutions, it is possible to describe the motion of atoms or molecules by solving Newton's equation of motion. The forces to which the particles are subjected are determined by means of specific interatomic potentials or force fields, and by relating the calculations of the forces and the motion of the particles, we are able to obtain detailed information about the motions and trajectories in the entire simulation process. Thus, by studying the total particle trajectories, molecular dynamics simulations provide us macroscopic information about the system under investigation through an analysis of the overall dynamic evolution [12]. Molecular Dynamics also helps us in understanding, at the atomic level, the mechanisms at the base of the charge storage and ion transport that take place in EDLCs: by studying the interaction between ions and ion pathways, we can obtain the distribution and motion of ions in the electrolyte, allowing us to obtain the dynamic behaviour and the resulting stored energy. This allows EDLCs based on nanomaterials to be studied more accurately, resulting in increasingly high-performance devices [12]. Although it is possible to perform MD simulations on different materials, the same type of approach that can be used for EDLCs cannot be fully applied in the study of reactions or pseudocapacities conversion processes, due to the lack of accurate reactive force field potentials [12]. In Molecular Dynamics simulations, the statistical ensemble representing the possible states of the system must also be defined. The states will vary their energy through contact with a heat bath at a fixed temperature. The main ensemble used in the literature is the so-called Canonical Ensemble NVT, whose variables determining the probability distribution of the states are the temperature T, the number of particles in the system N, and the volume V.

As mentioned above, simulations in Molecular Dynamics must necessarily start from potentials or force fields that describe the interactions between particles. In modelling carbon structures, there are many well-known empirical potentials: both non-reactive force fields such as molecular mechanics and reactive force fields such as Tersoff, REBO, ReaxFF, EDIP and LCBOP [18]. The ReaxFF (Reactive Force Field), a bond order-based force field that succeeds in modelling chemical reactions of continuous bond formation and breakage, is often used in the literature, taking into account atomic positions and considering both the contribution derived from direct reactions between atoms and the contribution derived from non-reactive interactions such as electrostatic or van der Waals

interactions. ReaxFF is based on empirical interatomic potentials and force fields from quantum mechanical structures and energy data such as heat of formation [22]. Although numerous simulations have been carried out using these potentials, the modelling of porous carbon structures is always problematic due to the fact that no potential can adequately combine the reactive chemical description of carbon bond formation/breakage with adequate computational efficiency. To overcome this problem, in some works, a reaction state summation (RSS) formalism is introduced in which all reactive states of the system are modelled separately via empirical non-reactive parameters. In this way, it is possible to study the individual reactive state in each case while maintaining the correct global physical description [18].

Unfortunately, few Molecular Dynamics simulations have been realised on Activated Carbon due to the difficulty of constructing a sufficiently representative numerical model of the complex structure [12].

One of the possible solutions is to use Quenched Molecular Dynamics (QMD) in which, starting with a regular initial approximate structure, thermal quenching is simulated on the model in order to obtain an amorphous carbon structure closer to reality [12]. After raising the temperature of the material above the value that induces a change of state, an abrupt cooling is performed that results in an amorphisation of the starting structure. Of course, even in the case of quenching as with normal Molecular Dynamics simulations, defining the initial boundary conditions as the process parameters is crucial. What is ultimately obtained is a qualitative study from quantitative parameters that helps in the understanding of experimental data, which is particularly useful in the study of nanoscale structures.

The aim of the analysis of simulations in Molecular Dynamics, and in Quenched Molecular Dynamics in particular, is to investigate the impact of varying initial parameters on the characteristics of the resulting structures. In order to improve the performance of EDLCs, this can be done by acting on the geometry of the electrodes, mainly by trying to obtain, as mentioned above, the greatest possible match between pore size and diameter of the ions in the electrolyte, and to better separate anions and cations, as in the case of supercapacitors with asymmetric electrodes. One can also act by increasing the quantum capacitance, by inserting heteroatoms or defects [12]. Molecular dynamics simulations can also involve the dynamics and ion pathway, which also depend to a large extent on the morphology of the electrode [12,13]. Among the various works in the literature reviewed, emphasis has been placed on those that provide more comprehensive data on porous amorphous carbon structures as a function of simulation

parameters, starting from well-known potentials and with great agreement with synthetic parameters. A first parameter of interest is certainly the Quench rate. What can be seen, analysing various studies examined, is that as the quench rate increases, the amorphisation of carbon structures increases [18, 19, 20, 21]. This result was expected, since if the quench rate is high, the atoms within the structure have very little time to organise themselves into an ordered configuration, resulting in an amorphous structure. Conversely, if the quench rate decreases, the atoms have more time to reconfigure themselves into more crystalline structures. This can also produce an increase in the final density relative to the initial density as a function of the decrease in the quenching rate, but very slight [18, 19]. At low quench rates, the Specific Surface Area (SSA) decreases [21]. As the quenching rate decreases, there is also an increase in pore size because slower cooling induces fewer defects in the final structure in which the carbon flakes are more planar and therefore aggregate to form larger pores [18]. The carbon bonds appear more in accordance with the experimental data but, as we have said, we obtain larger pores than we would like to obtain for nanometric structures. In some cases, as in study [19], a compression step is added to the simulations in order to obtain smaller pores. The absorption of chemical species is also influenced by the Quench rate, as it depends on the structure and volume of the accessible pores. In particular, the amount of atoms absorbed increases monotonically with structural order and thus with lower quench rates, although the pore size decreases [21].

Table 7 and figure 24 and 25 show the effect of varying the quench rate on the parametric and configurations for QMD samples from the study [18] in which simulations were carried out on porous carbon models consisting of graphene layers.

Samples	$\rho_{initial}$ (atoms/Å^3)	$T_{initial}$ (10^4 K)	T_{final} (10^4 K)	Quench time (ps)	Quench rate (10^{12} K/s)
CS400	0.0580	2.1	0.66	140	102
CS1000	0.0765	2.1	0.66	2100	6.81
CS1000a	0.0380	1.5	0.66	3200	2.64

Table 7. Procedures to prepare CS400, CS1000, and CS1000a samples in work [18].
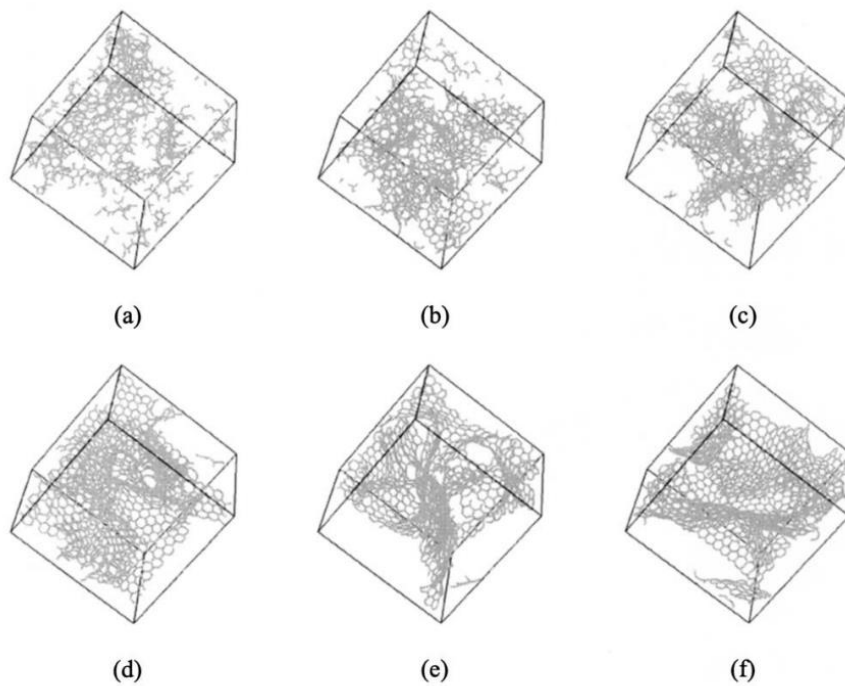
Figure 24. Atomic configurations for QMD samples with different quench rate. The quench rate decreases from (a) to (f) . Bonds are built for any two carbon atoms with a distance smaller than 1.8 Å [18].
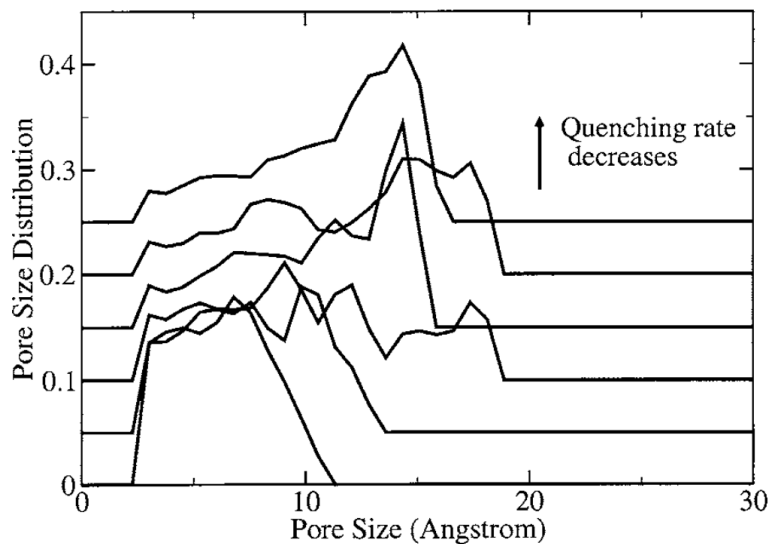
Figure 25. Pore size distribution functions for QMD samples with different quench rate. The curves are shifted vertically for clarity [18].

Table 8 and Figure 26, 27 show the variation of the quench rate on the parameters and structures of the study [19] in which real nanoporous carbide-derived carbons (CDCs) structures are simulated. As mentioned above, an additional compression process is also added to some of the simulated samples in order to decrease the pore size.

Sample	Q, K ps^{-1}	$\bar{p}$, nm	L, nm	ρ, g cm^{-3}	Compression
QMD-100	100	0.50	7.488	0.950	No
QMD-10	10	0.97	7.488	0.950	No
QMD-10c	10	0.56	6.489	1.467	Yes
QMD-1	1	1.40	7.488	0.950	No
QMD-1c	1	0.91	6.733	1.311	Yes

Table 8. Summary of sample structures. Models are named 'QMD-x' where 'x' is the quench rate used to produce it (in units of 1 K ps^{-1}–100 K ps^{-1}). A 'c' is appended to the name if a post-quench compression step was included. Q: Quench rate, K ps^{-1} ; $\bar{p}$: mean pore size, nm; L: Box length, nm; ρ: Particle density, g cm^{-3} [19].

(a) QMD-100   (b) QMD-10   (c) QMD-1

(d) QMD-10c   (e) QMD-1c
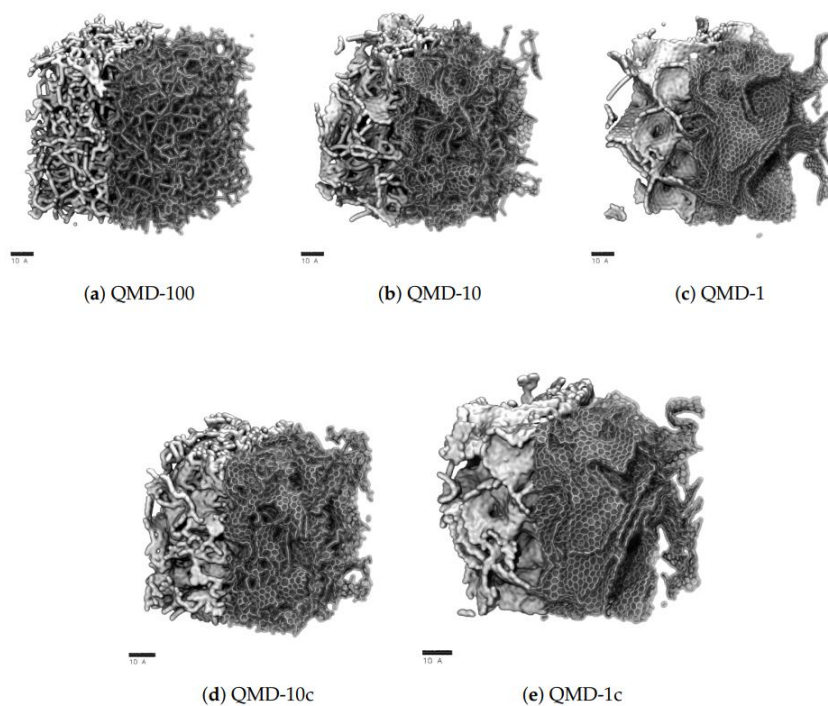
Figure 26. Sample structures produced via quenched molecular dynamics (QMD) at quench rates and comparison to STEM of Si-CDC from experiment. Simulation boxes are between 6.5 and 7.5 nm in length and include 20,000 atoms. Each scale bar is 10 Å or 1 nm long [19].
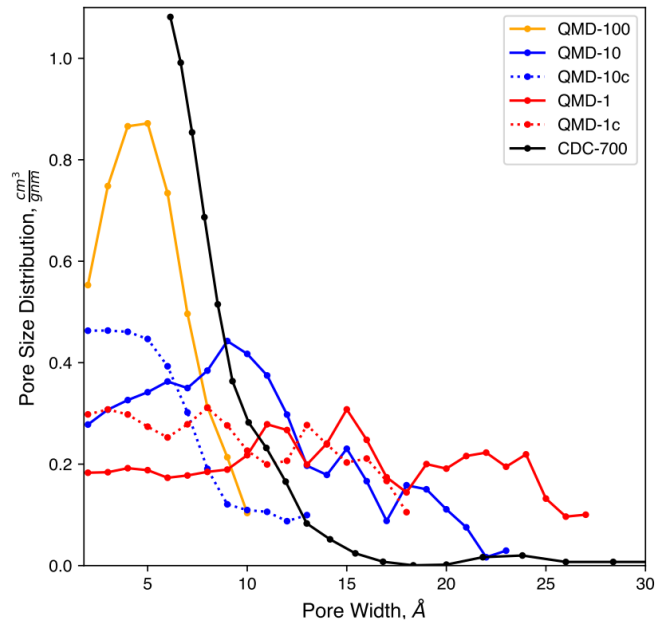
Figure 27. Pore size distributions of model samples compared to experiments [19].

Remaining on CDC structures, the study [21] shows the comparison between Molecular Dynamics simulations and synthetic samples of TiC as precursor using different chlorination temperatures. The quenchig rate, in order to modulate the structures in the final models, is systematically varied from 160×10^{12} K/s to 2.5×10^{12} K/s by a factor of 2, to achieve a relative range of 64x to 1x. The initial carbon density in the simulation cell is chosen so that the final density is approximately constant at 0.94 g/cm^3 (Table 9). Figures 28, 29 and 30 shows the comparison between experimental data and simulations.

Relative quench rate, r_{quench}	Initial density, ρ_o (g/cm^3)	Final density, ρ_f (g/cm^3)	Unit cell length, L (nm)
64x	1.114	0.943	4.15
32x	1.057	0.944	4.22
16x	1.011	0.935	4.29
8x	0.983	0.939	4.33
4x	0.955	0.945	4.36
2x	0.965	0.941	4.36
1x	0.957	0.941	4.37

Table 9. Summary of simulation parameters used to generate the model structures [21].
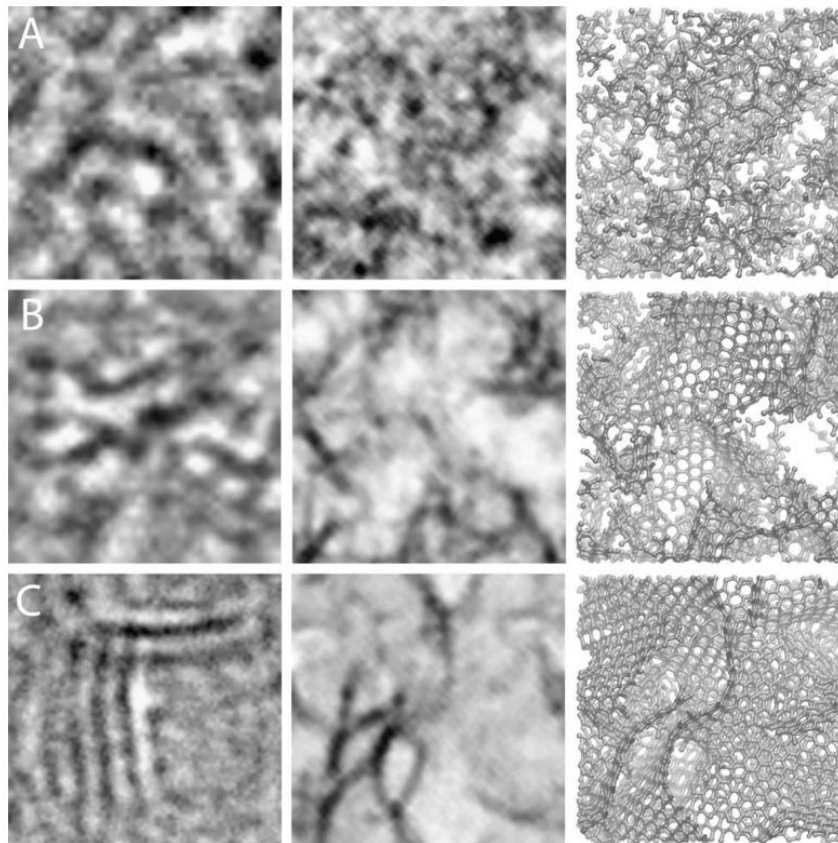
Figure 28. Comparison of experimental HRTEM images (left column), simulated HRTEM images (center column) and snapshots of the model structures (right column). Each images has been scaled such that the edge length corresponds to 4 nm. (A) HRTEM images of Ti-CDC synthesized at 600 °C and QMD structure quenched at 64x, respectively. (B) Same as (A) except for 800 °C and 8x. (C) Same as (A) except for 1200 °C and 1x [21].
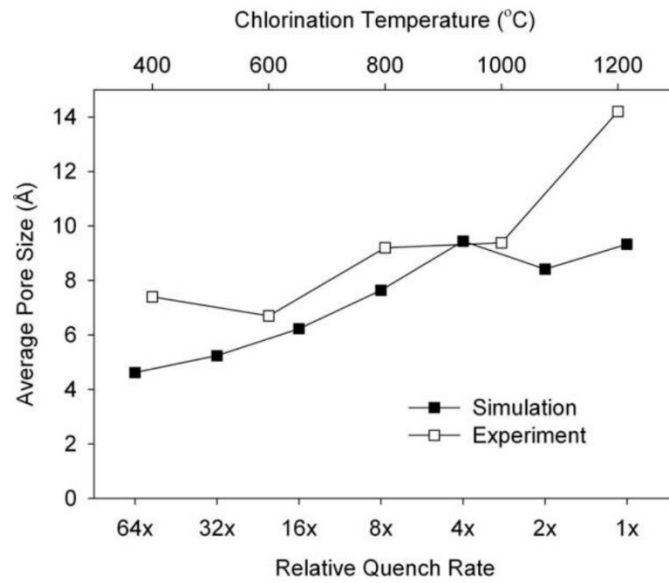
Figure 29. Average pore size as a function of relative quench rate (simulation) and chlorination temperature (experiment) [21].
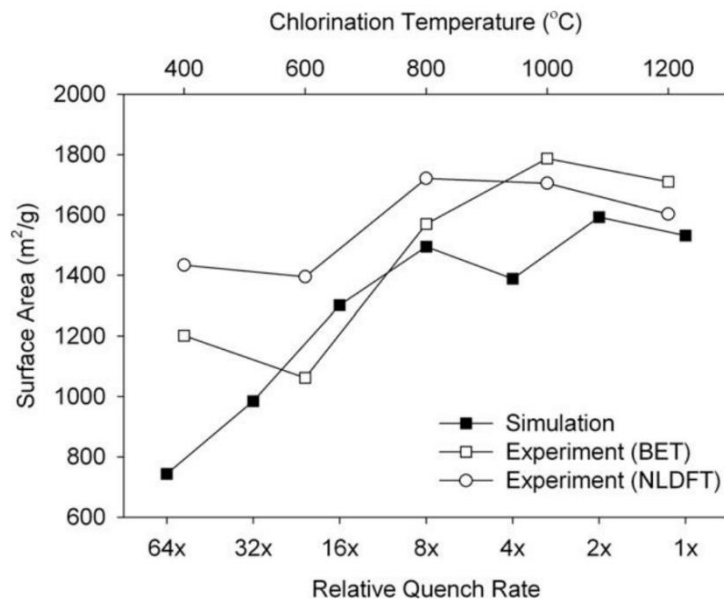
Figure 30. Specific surface area as a function of relative quench rate (simulation) and chlorination temperature (experiment) [21].

As mentioned earlier, the amount of chemical species absorbed increases monotonically with higher structural order at low quench rates, although this leads to a reduction in pore size. In the case of the study [21] it is shown that this is due to the effective interaction between Argon and Carbon increasing due to more crystalline structural bonds as a result of a higher local density in the carbon matrix (figures 31 and 32).
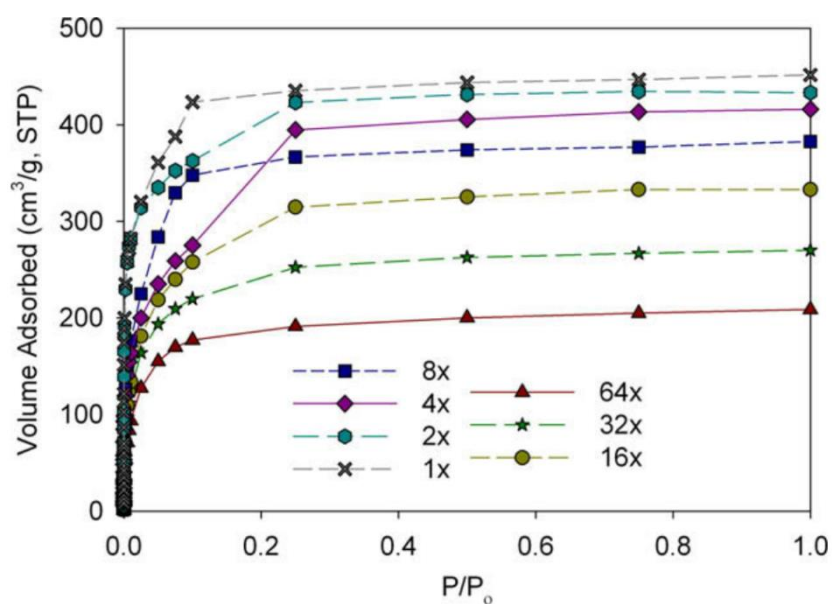
Figure 31. Argon adsorption isotherms at 77 K for QMD-generated structures [21].
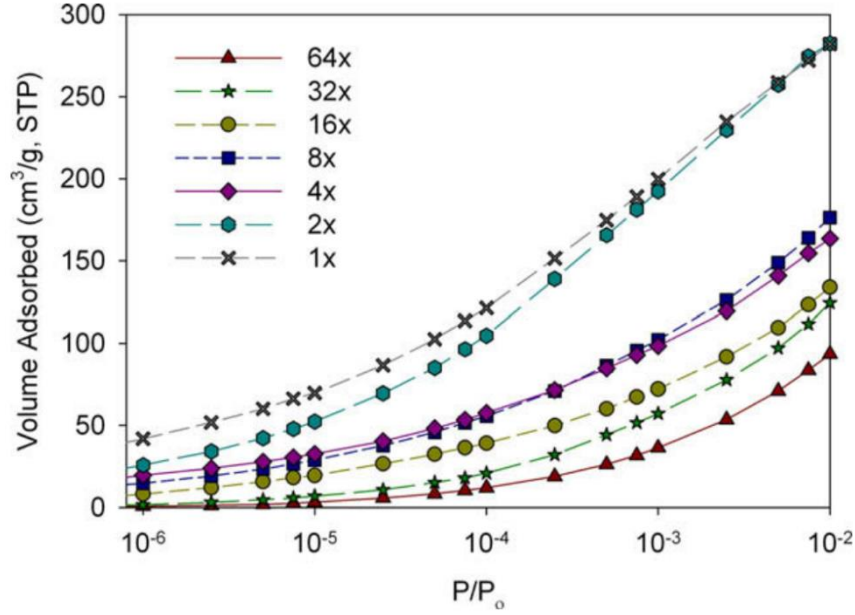
Figure 32. Argon adsorption isotherms at 77 K for QMD-generated structures in log-scale to show the low pressure region [21].

In the study [20], the synthesis and characterisation of a Glassy Carbon (GC), a carbon structure formed from curved graphene-shaped carbon flakes, is analysed using molecular dynamics. What is further highlighted here is that the holding time, i.e. the duration for which the structure is held at a temperature close to the phase change, greatly influences the structural order: a short holding phase will lead to a higher degree of graphitisation (Figure 34). The maximum temperature of the holding phase will also influence the final structure: a higher temperature will lead to easier breaking of atomic bonds and subsequent difficult recombination, resulting in an amorphous structure (Figures 33 and 34). Table 10 shows the simulation parameters, while the following figures show the different structures simulated.

Case	T_{max} (K)	t_{ramp} (ps)	ramping rate (K/ps)	t_{hold} (ps)	t_{cool} (ps)	cooling rate (K/ps)	t_{total} (ps)
GC^0	3100	400	7.0	1750	280	10	2430
GC^{Ext}	3100	400	7.0	3250	560	20	4210
GC^{LT} ('*low-temp*')	2400	260	8.1	2050	210	10	2520
GC^{HT1} ('*high-temp*')	3250	445	6.6	825	295	10	1565
GC^{HT2} ('*high-temp*')	3700	520	6.5	400	340	10	1260

Table 10. Summary of simulation sets used [20].
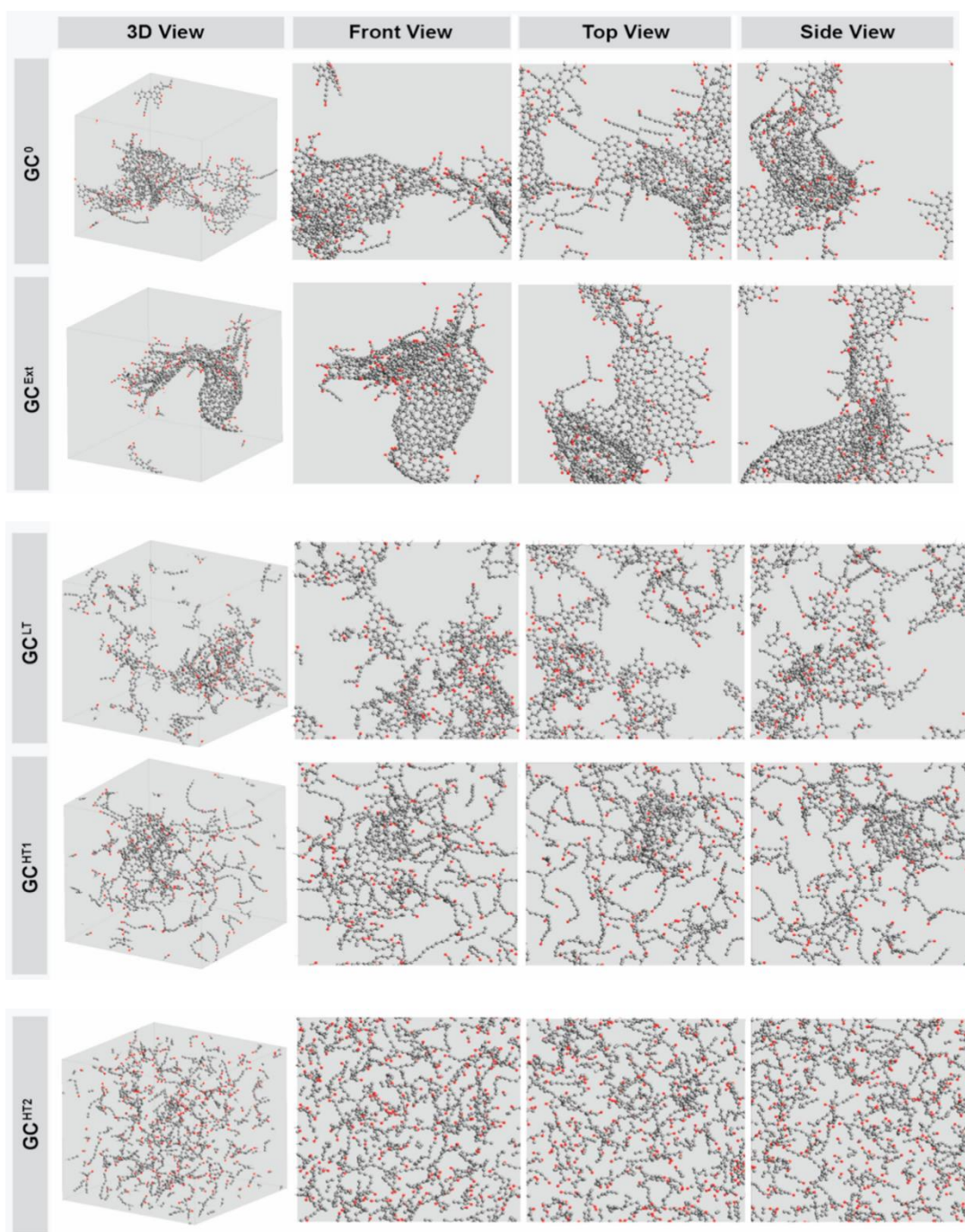
Figure 33. Final carbon structures for the 3100 K (GC[0] & GC[Ext]), 2400 K (GC[LT]) (GC[HT1]), and 3700 K (GC[HT2]) simulations. Interconnected and curved layers form tube-like, 3D closed-cage nanostructures in GC0 and GC[Ext] cases, however no clear formation of complex nanostructures are observed in the other cases [20].
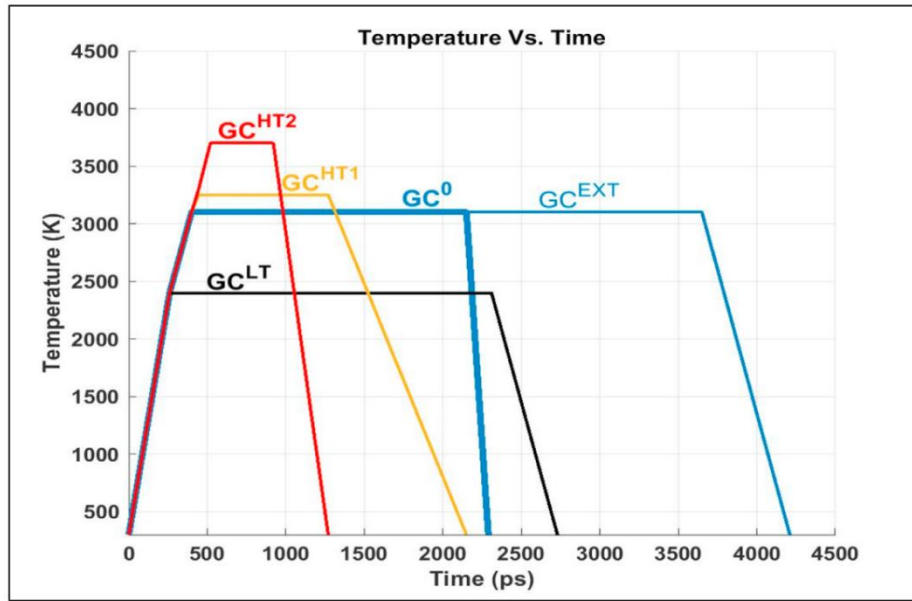
Figure 34. Temperature and time profile of the 5 cases (3 sets) considered for simulation, i.e., (GC^0 , GC^{Ext}), GC^{LT}, and (GC^{HT1}, GC^{HT2}) [20].

Another parameter to evaluate is the initial density of the structure and its influence on the final density. What is observed is that at lower initial densities, we obtain a lower final density, as we would expect, with a more amorphous structure and also a slight increase in porosity [18]. This is due to the lower amount of atoms in the initial structure, which therefore have more space to create a more crystalline configuration with larger pores (Figures 35 and 36). The increase in porosity can be mitigated by a subsequent compression step as described previously (Figure37) [19]. The fractal size on the other hand, i.e. the average number of atoms present within a distance r from a central atom, increases significantly as the final density increases, again due to a higher initial concentration of atoms (Figure 38) [18].
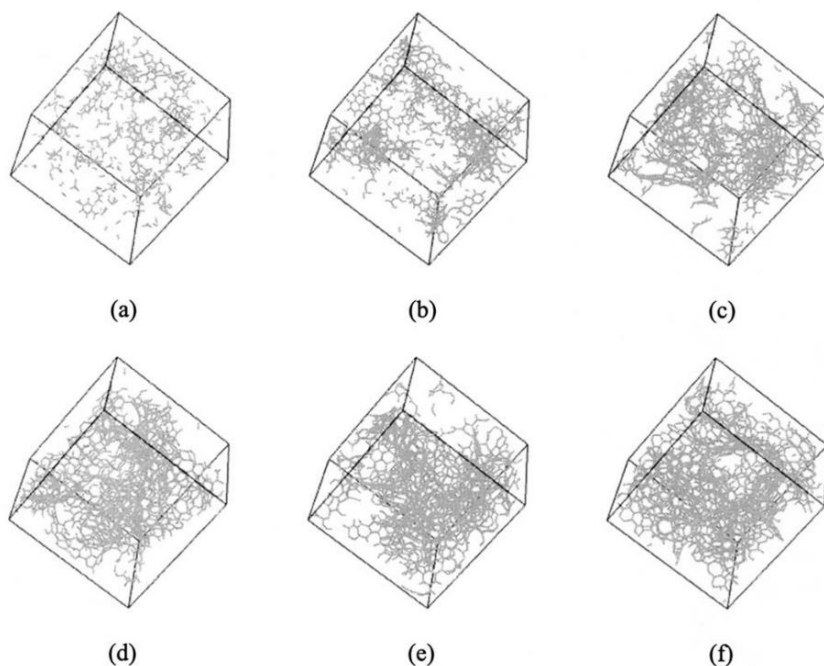
Figure 35. Atomic configurations for QMD samples with different initial density in work [18]. The initial density increases from (a) to (f). Bonds are built for any two carbon atoms with a distance smaller than 1.8 Å.
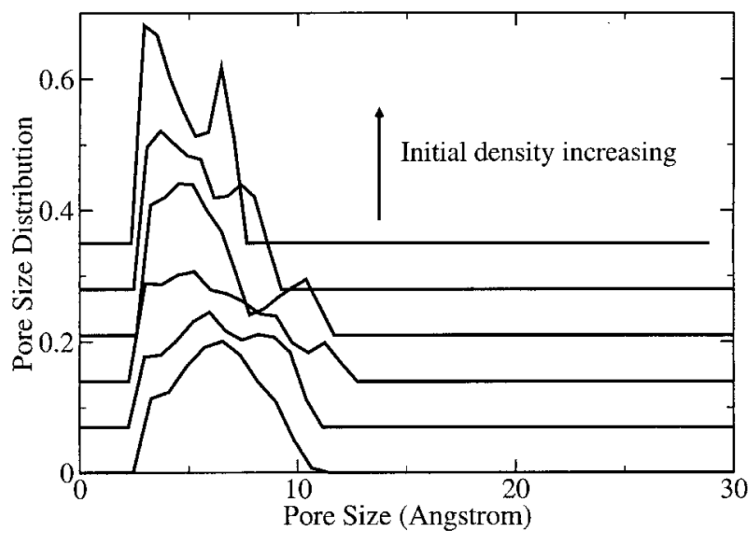
Figure 36. Pore size distribution functions for QMD samples with different initial density in [18]. The curves are shifted vertically for clarity.
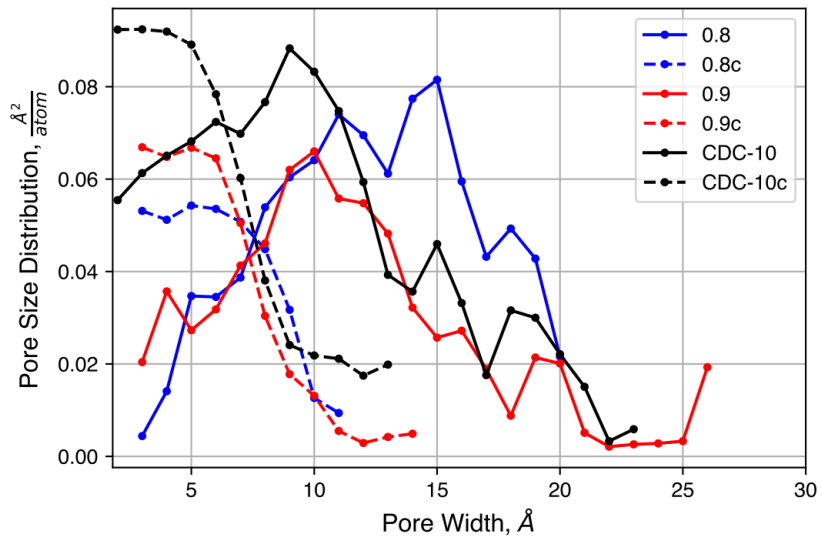
Figure 37. Pore size distributions of samples with decreased initial density, before and after compression [19].
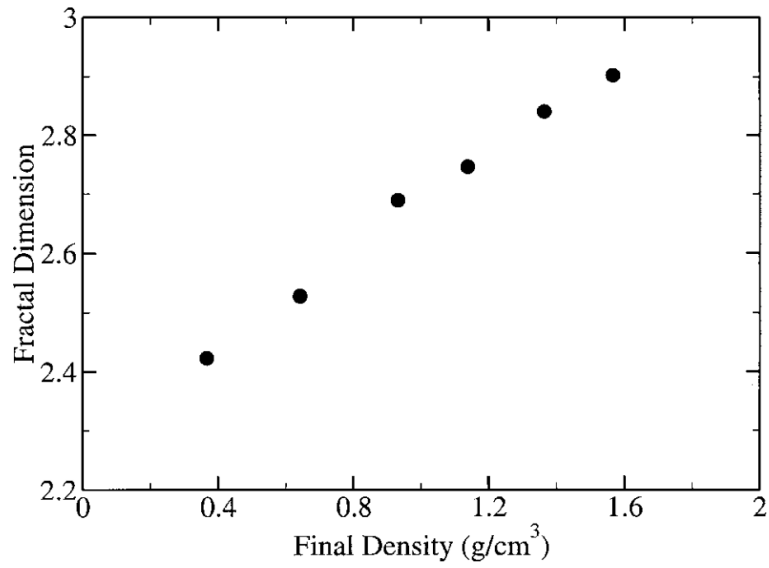
Figure 38. Fractal dimension as a function of final density of the porous carbon samples obtained from QMD method [18].

Conclusion

As we have seen in this discussion, the carbon-based structures used to make the cell's electrodes are crucial in supercapacitive EDLC applications. The goal is to obtain amorphous structures with the right degree of porosity and pore size, so as to have the best possible match with the size of the electrolyte ions. It is also essential to maximise the contact area between electrode and electrolyte in order to have the highest possible ion exchange surface area. As mentioned, due to the amorphous nature of structures of this type, the main problem is the difficulty in studying and characterising the experimental structures, which present a mainly short-range order, which is complex to define accurately. The description of some structural characteristics is even, in some cases, only possible through simulative processes. In these cases, only general trends are derived, which are then indirectly used in the understanding of synthesised structures. The study of real structures must, therefore, follow hand in hand with the realisation of simulated structures to increase understanding of material behaviour at the nanoscale. Among the various simulative algorithmic techniques in the literature, molecular dynamics appears to be one of the best approaches for such a route. In particular, using a quenching step allows amorphous structures to be obtained from more crystalline and thus more easily defined models. Studying the various cases, what emerges is that the main problem always remains that of defining a suitable potential in the simulations of structures. The potential used must first be as capable as possible of representing the real evolution of the particles that make up the synthesis structures, but at the same time must not require such computational complexity that it cannot be used in practice. One of the main limitations of simulations in matching experimental data, however, remains the lack of a potential that takes into account long-range dispersion forces between unbound carbon atoms. The potentials used generally only take into account short-range interactions between bonded atoms. The search for the best potential to be used in the simulation process, therefore, remains the main objective in the characterisation of carbon structures for electrodes. In addition, as can be seen from the cases examined, using quenching in molecular dynamics simulations is a great ally in obtaining structures more similar to real amorphous ones. However, even in this case, it must be borne in mind that by changing the quenching parameters (such as the rate or retention time), a compromise must be found between the accuracy of defining atomic bonds and obtaining a suitably amorphous structure as in synthetic processes. The initial simulation parameters also play an important role (first and foremost the density), and the initial structure under consideration must therefore be carefully defined so that the comparison between simulation and reality is as accurate as possible. In

conclusion, future perspectives on the study of carbon structures will require further developments with regard to the realisation of increasingly efficient algorithms to be used in simulation techniques and the definition of potentials that are as accurate as possible in representing the dynamics at play in the structures under examination.

Bibliography

[1] **M. Pershaanaa, Shahid Bashir, S. Ramesh, K. Ramesh,** Every bite of Supercap: A brief review on construction and enhancement of supercapacitor, Journal of Energy Storage 50 (2022) 104599, https://doi.org/10.1016/j.est.2022.104599

[2] **Li Li Zhang and X. S. Zhao,** Carbon-based materials as supercapacitor electrodes, Chemical Society Reviews, 2009, 38, 2520–2531, Carbon-based materials as supercapacitor electrodes - Chemical Society Reviews (RSC Publishing)

[3] **Soheila Faraji, Farid Nasir Ani,** The development supercapacitor from activated carbon by electroless plating—A review, Renewable and Sustainable Energy Reviews 42 (2015) 823–834, https://doi.org/10.1016/j.rser.2014.10.068

[4] **Saswata Bose, Tapas Kuila, Ananta Kumar Mishra, R. Rajasekar, Nam Hoon Kimc and Joong Hee Lee,** Carbon-based nanostructured materials and their composites as supercapacitor electrodes, J. Mater. Chem., 2012, 22, 767, https://doi.org/10.1039/C1JM14468E

[5] **Sumaiyah Najib and Emre Erdem,** Current progress achieved in novel materials for supercapacitor electrodes: mini review, Nanoscale Adv., 2019, 1, 2817, https://doi.org/10.1039/C9NA00345B

[6] **Lihong Wang, Masahito Fujita, Michio Inagaki**, Relationship between pore surface areas and electric double layer capacitance in non-aqueous electrolytes for air-oxidized carbon spheres, Electrochimica Acta 51 (2006) 4096–4102, 10.1016/j.electacta.2005.11.039

[7] **Lihong Wang, Takahiro Morishita, Masahiro Toyoda, Michio Inagaki,** Asymmetric electric double layer capacitors using carbon electrodes with different pore size distributions, Electrochimica Acta 53 (2007) 882–886, 10.1016/j.electacta.2007.07.069

[8] **Justin N. Neala, David J. Wesolowskib, Douglas Hendersonc, Jianzhong Wu,** Electric double layer capacitance for ionic liquids in nanoporous electrodes: Effects of pore size and ion composition, Journal of Molecular Liquids 270 (2018) 145–150, https://doi.org/10.1016/j.molliq.2017.10.128

[9] **Chen Li, Xiong Zhang, Kai Wang, Fangyuan Su, Cheng-Meng Chen, Fangyan Liu, Zhong-Shuai Wu, Yanwei Ma,** Recent advances in carbon nanostructures prepared from carbon dioxide for high-performance

supercapacitors, Journal of Energy Chemistry 54 (2021) 352–367, https://doi.org/10.1016/j.jechem.2020.05.058

[10] **Elzbieta Frackowiak,** Carbon materials for supercapacitor application, Phys. Chem. Chem. Phys., 2007, 9, 1774–1785, https://doi.org/10.1039/B618139M

[11] **Marta Sevilla, Robert Mokaya,** Energy storage applications of activated carbons: supercapacitors and hydrogen storage, Energy Environ. Sci., 2014, 7, 1250–1280, https://doi.org/10.1039/C3EE43525C

[12] **Zheng Bo, Changwen Li, Huachao Yang, Kostya Ostrikov, Jianhua Yan, Kefa Cen,** Design of Supercapacitor Electrodes Using Molecular Dynamics Simulations, Nano-Micro Lett. (2018) 10:33, https://doi.org/10.1007/s40820-018-0188-2

[13] **N.N. Rajput, J. Monk, F.R. Hung**, Ionic liquids confined in a realistic activated carbon model: a molecular simulation study, J. Phys. Chem. C 118(3), 1540–1553 (2014). https://doi.org/10.

[14] **Ander González, Eider Goikolea, Jon Andoni Barrena, Roman Mysyk,** Review on supercapacitors: Technologies and materials, Renewable and Sustainable Energy Reviews 58 (2016) 1189–1206, http://dx.doi.org/10.1016/j.rser.2015.12.249

[15] **Guoping Wang, Lei Zhang and Jiujun Zhang,** A review of electrode materials for electrochemical supercapacitors, Chem. Soc. Rev., 2012, 41, 797–828, https://doi.org/10.1039/C1CS15060J

[16] **Thilageshwaran Subramaniam , Mohamed Ansari Mohamed Nainar, Noor Afeefah Nordin,** A Review on Synthesis and Characterization of Activated Carbon from Natural Fibers for Supercapacitor Application, Pertanika J. Sci. & Technol. 30 (1): 351 - 376 (2022), https://doi.org/10.47836/pjst.30.1.20

[17] **Parveen Saini,** A Historical Review of Electrode Materials and Electrolytes for Electrochemical Double Layer Supercapacitors and Pseudocapacitors, Indian Journal of Pure & Applied Physics Vol. 61, April 2023, pp. 268-290, https://doi.org/10.56042/ijpap.v61i4.69622

[18] **Yunfeng Shi,** A mimetic porous carbon model by quench molecular dynamics simulation, J. Chem. Phys. 128, 234707 (2008), https://doi.org/10.1063/1.2943645

[19] **Matthew W. Thompson, Boris Dyatkin, Hsiu-Wen Wang, C. Heath Turner, Xiahan Sang, Raymond R. Unocic, Christopher R. Iacovella, Yury**

Gogotsi, Adri C. T. van Duin, Peter T. Cummings, An Atomistic Carbide-Derived Carbon Model Generated Using ReaxFF-Based Quenched Molecular Dynamics, Journal of Carbon Research *C* **2017**, *3*(4), 32, https://doi.org/10.3390/c3040032

[20] **Rhea Montgomery-Walsh, Surabhi Nimbalkar, James Bunnell, Sandra Lara Galindo, Sam Kassegne**, Molecular dynamics simulation of evolution of nanostructures and functional groups in glassy carbon under pyrolysis, Carbon 184 (2021) 627e640, https://doi.org/10.1016/j.carbon.2021.08.070

[21] **J.C. Palmer, A. Llobet, S.-H. Yeon, J.E. Fischer, Y. Shi, Y. Gogotsi, K.E. Gubbins,** Modeling the structural evolution of carbide-derived carbons using quenched molecular dynamics, CARBON 48 (2010) 1116 – 1123, https://doi.org/10.1016/j.carbon.2009.11.033

[22] **Surabhi Nimbalkar, Rhea Montgomery-Walsh, James Bunnell, Sandra Lara Galindo, Brinda Kodira Cariappa, Abhivyakti Gautam, Rene Arvizu, Shize Yang, Sam Kassegne,** Carbon allotropes form a hybrid material: Synthesis, characterization, and molecular dynamics simulation of novel graphene-glassy carbon hybrid material, Carbon 196 (2022) 1012–1023, https://doi.org/10.1016/j.carbon.2022.05.049